

Macrocylic Ligands

Bifunctional Cyclam-Based Ligands with Phosphorus Acid Pendant Moieties for Radiocopper Separation: Thermodynamic and Kinetic Studies

Monika Paúrová,^[a] Jana Havlíčková,^[a] Aneta Pospíšilová,^[b] Miroslav Vetrík,^[b] Ivana Císařová,^[a] Holger Stephan,^[c] Hans-Jürgen Pietzsch,^[c] Martin Hrubý,^[b] Petr Hermann,^[a] and Jan Kotek*^[a]

Abstract: Two macrocyclic ligands based on cyclam with *trans*-disposed *N*-methyl and *N*-(4-aminobenzyl) substituents as well as two methylphosphinic (H₂L1) or methylphosphonic (H₄L2) acid pendant arms were synthesised and investigated in solution. The ligands form stable complexes with transition metal ions. Both ligands show high thermodynamic selectivity for divalent copper over nickel(II) and zinc(II)— $K(\text{CuL})$ is larger than $K(\text{Ni/ZnL})$ by about seven orders of magnitude. Complexation is significantly faster for the phosphonate ligand H₄L2, probably due to the stronger coordination ability of the more basic phosphonate groups, which efficiently bind the metal ion in an “out-of-cage” complex and thus accelerate its “in-cage” binding. The rate of Cu^{II} complexation by the phosphinate ligand H₂L1 is comparable to that of cyclam itself and its derivatives with non-coordinating substituents. Acid-assisted decomplexation of the copper(II) complexes is relatively fast ($\tau_{1/2} = 44$ and 42 s

in 1 M aq. HClO₄ at 25 °C for H₂L1 and H₄L2, respectively). This combination of properties is convenient for selective copper removal/purification. Thus, the title ligands were employed in the preparation of ion-selective resins for radiocopper(II) separation. Glycidyl methacrylate copolymer beads were modified with the ligands through a diazotisation reaction. The separation ability of the modified polymers was tested with cold copper(II) and non-carrier-added ⁶⁴Cu in the presence of a large excess of both nickel(II) and zinc(II). The experiments exhibited high overall separation efficiency leading to 60–70% recovery of radiocopper with high selectivity over the other metal ions, which were originally present in 900-fold molar excess. The results showed that chelating resins with properly tuned selectivity of their complexing moieties can be employed for radiocopper separation.

Introduction

The investigation of thermodynamically highly stable and kinetically inert complexes (often formed by macrocyclic ligands)^[1–3] has been stimulated by their applications in several areas, for example, as contrast agents in magnetic resonance imaging^[4–8] and for labelling of biomolecules with metal radioisotopes for both diagnostic and therapeutic purposes.^[9–18]

Some copper radioisotopes, for example, ⁶¹Cu (half-life $\tau_{1/2} = 3.33$ h, β^+ emitter), ⁶⁴Cu ($\tau_{1/2} = 12.7$ h, β^+ and β^- emitter) and ⁶⁷Cu ($\tau_{1/2} = 61.8$ h, β^- emitter), exhibit a great potential for both diagnosis (positron emission tomography) and therapy (β^- particles of intermediate energy).^[9,19–21] Among them, ⁶⁴Cu has the greatest importance due to its theranostic character. All of these isotopes are usually produced by proton irradiation in cyclotrons. Isotope ⁶¹Cu is usually produced by irradiation of a natural zinc target (⁶⁴Zn(p, α)⁶¹Cu reaction),^[22] and ⁶⁷Cu by the ⁶⁸Zn(p,2p)⁶⁷Cu process, while the most common method to produce ⁶⁴Cu is irradiation of an isotopically enriched nickel target (⁶⁴Ni(p,n)⁶⁴Cu reaction). In all cases, separation of copper radionuclides from a large excess of the Zn or Ni target material is required and, in the case of isotopically enriched ⁶⁴Ni targets, recovery of the nickel isotope is essential to production economics. For the production of non-carrier-added (NCA) copper radioisotopes, simple ion-exchange techniques are the most common.^[23] Recently, Dirks et al. described the separation of Cu from a Ni target by a solid-phase extraction technique and demonstrated that macroscopic amounts of Zn do not reduce the retention of Cu. However, the chemical composition of the resin was not published.^[24] Therefore, research focused on new ligands for copper(II) to tune the properties of

[a] M. Paúrová, J. Havlíčková, Dr. I. Císařová, Prof. P. Hermann, Prof. J. Kotek
Department of Inorganic Chemistry
Faculty of Science, Universita Karlova (Charles University)
Hlavova 2030, 12840 Prague 2 (Czech Republic)
E-mail: modrej@natur.cuni.cz

[b] A. Pospíšilová, M. Vetrík, Dr. M. Hrubý
Institute of Macromolecular Chemistry
The Academy of Sciences of the Czech Republic
Heyrovského náměstí 2, 16206 Prague 6 (Czech Republic)

[c] Dr. H. Stephan, Dr. H.-J. Pietzsch
Helmholtz-Zentrum Dresden-Rossendorf
Institute of Radiopharmaceutical Cancer Research
Bautzner Landstraße 400, 01328 Dresden (Germany)

Supporting information for this article is available on the WWW under <http://dx.doi.org/10.1002/chem.201405777>.

both ligands and their complexes is a vital part of coordination chemistry. Ligands with very high selectivity for Cu^{II} over Ni^{II}/Zn^{II} are desired for radiomedicinal purposes.

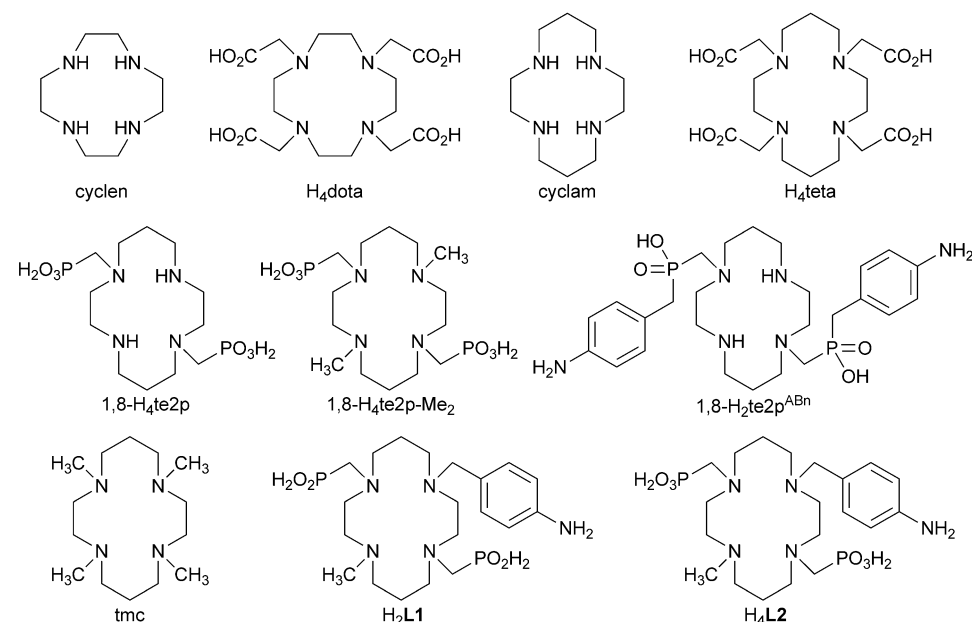
Some time ago, we started investigations of cyclam-based ligands containing phosphorus acid pendant arms,^[25–36] which are suitable for complexation of the first-row transition metal ions. Optimal properties are exhibited especially by ligands having six donor atoms (i.e., with two coordinating pendant arms). Because of their strong complexing ability, phosphorus acid groups seem to significantly accelerate the complexation reaction because, taking into account the common complexation mechanism of macrocyclic chelators, they form rather stable initial “out-of-cage” complexes that further rearrange to “in-cage” complexes (i.e., the central metal ion is coordinated by all nitrogen atoms of the macrocyclic unit). It has been observed that fully *N*-substituted cyclam derivatives (i.e., only tertiary amino groups are present) have significantly different properties; in particular, their complexes show significantly lower kinetic inertness than those of ligands having one or

tested for separation of ⁶⁴Cu from the expected metal-ion impurities Ni^{II} and Zn^{II}, to show that preparation and utilisation of such selective chelating resins in radiochemistry is feasible.

Results and Discussion

Synthesis

Selective 1,8-disubstitution of the cyclam ring by two different groups can be achieved by stepwise alkylation of cyclam–formaldehyde or cyclam–glyoxal bis-aminals followed by alkaline hydrolysis of the resulting bis-quaternary intermediates.^[37–40] In such alkylation reactions, cyclam–formaldehyde bis-aminal **1** is more reactive and quaternisation steps proceed fast. However, although several mono-quaternary intermediates have been isolated, and compound **1** has been successfully employed for synthesis of some non-symmetrically substituted cyclams,^[38,41–43] in our case, only mixtures of mono- and bis-quaternised aminals were isolated after reaction with the first alkylating agent: using methyl iodide or *p*-nitrobenzyl bromide gave the same result. Therefore, the required unsymmetrical bis-quaternary salt was always contaminated by the symmetrical one originating from the first reaction step. Thus, symmetrically substituted 1,8-di-methyl or 1,8-bis(*p*-nitrobenzyl) cyclams were isolated as by-products after hydrolysis of the crude (impure) bis-quaternary salts (Supporting Information, Scheme S1), and isolation of the product **5** required chromatographic separation. One of the by-products, namely, 1,8-bis(*p*-nitrobenzyl)cyclam, was structurally characterised by single-crystal X-ray diffraction (Supporting Information, Figure S1).



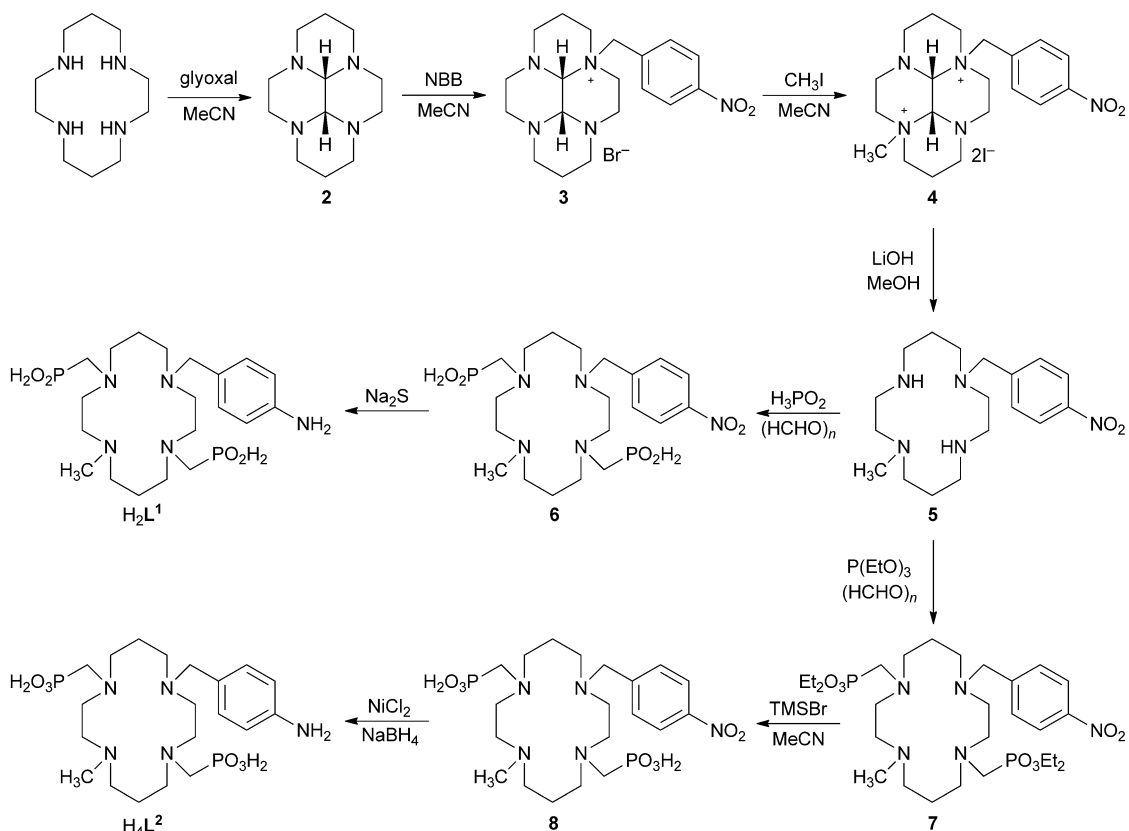
Scheme 1. Structures of ligands mentioned in the text.

more secondary amino groups. Previously, we have shown that the ligand 1,8-H₄te2p-Me₂ (Scheme 1) forms a copper(II) complex with very high selectivity, and acid-assisted dissociation of the complex is faster than that observed for non-methylated derivative 1,8-H₄te2p.^[35]

Thus, we consider that analogous ligands and their conjugates can be employed for selective copper(II) separation from other metal ions, which can be coupled with the possibility to recover copper(II) by using strong acids. Herein, we report on coordinating properties of 4-methyl-11-(*p*-aminobenzyl)cyclam-based ligands with two methylphosphinic or methylphosphonic acid pendant arms (H₂L1 and H₄L2, respectively; Scheme 1). The ligands were conjugated with a hydrophilic polymer and

For the above reasons, cyclam–glyoxal *cis*-bis-aminal **2** was employed in the quaternisation reactions (Scheme 2).^[33,39] In this case, monoquaternary salts can be isolated in pure form, because the difference in reactivity between the first and second alkylation steps is significant.

The reaction of a monomethyl quaternary aminal with *p*-nitrobenzyl bromide is extremely slow, and therefore the reverse strategy was used. First, the mono(*p*-nitrobenzyl) quaternary salt **3** was isolated,^[33] and a suspension thereof in acetonitrile was allowed to react with a large excess of methyl iodide for two weeks at room temperature to afford bis-quaternary salt **4**, the identity of which was confirmed by X-ray diffraction (Supporting Information, Figure S2). Surprisingly, in the second alkylation step, bromide/iodide anion exchange was observed



Scheme 2. Synthesis of H_2L1 and H_4L2 .

and was also confirmed by elemental analysis of the bulk material.

The kind of base used in the next, hydrolytic step is crucial; when NaOH or KOH was used, elimination of *p*-nitrobenzyl group was observed, and it was followed by further reactions and, according to TLC, several (unidentified) by-products were formed besides the required disubstituted cyclam **5**. In these cases, isolation of amine **5** required chromatography, and the yields of isolated product were rather low (ca. 50%). This problem was solved by using LiOH, with which the hydrolysis proceeded without side reactions, and the required product **5** was isolated almost quantitatively after a simple extraction. Compound **5** is a crystalline solid, and its identity was unambiguously confirmed by single-crystal X-ray diffraction (Supporting Information, Figure S3). Although the molecule of **5** is partly disordered, it is clear that the macrocycle adopts an unusual geometry related to Bosnich conformation $V^{[1,44]}$

In further reaction steps, phosphorus acid pendant arms were introduced by Mannich-type reactions between amine **5**, formaldehyde and hypophosphorous acid (leading to compound **6** after purification by ion-exchange chromatography) or triethyl phosphite (affording isolated intermediate ester **7**, which was hydrolysed through trimethylsilyl bromide transesterification to give compound **8**). The aromatic nitro group of compounds **6** and **8** was then reduced to an amino group by sodium sulfide and Raney nickel-catalyzed reduction with borohydride, respectively. Ligands H_2L1 and H_4L2 were isolated in zwitterionic form after ion-exchange chromatography

(strong cation-exchange resin, elution with pyridine) in oily/glassy forms.

On mixing ligands H_2L1 and H_4L2 with solutions of Cu^{II} salts, fast complexation proceeds with an immediate colour change to deep green. The Cu^{II} complexes of both ligands were found to be stable towards isomerisation, since neither UV/Vis spectral changes nor new TLC spot(s) were observed after heating slightly acidic, neutral or alkaline aqueous solutions of the complexes to reflux for 2 d or allowing the stock solutions of the complexes to stand at room temperature for several months.

Thermodynamic properties

Thermodynamic properties of H_2L1 and H_4L2 and their complexes were studied by potentiometric titration. Protonation constants of the free ligands are in the expected range of values reported for related compounds (Table 1 and Supporting Information, Table S1), and the corresponding distribution diagrams are shown in Figure 1. Starting from fully deprotonated species $L1^{2-}$ and $L2^{4-}$, the first two protonation steps, which are characterised by $\log K_f$ values of 10.32 and 9.87 to give $HL1^-$ and H_2L1 species, and 11.43 and 11.42 to give $HL2^{3-}$ and H_2L2^{2-} , respectively, correspond to protonation of the amino groups of the macrocycle. The doubly protonated cyclam skeleton is locked in a stable conformation due to the presence of intramolecular hydrogen bonds.^[1] In cyclam itself and in several of its derivatives, such hydrogen bonds even

Table 1. Stepwise protonation constants $\log K_h^{[a]}$ of H_2L1 and H_4L2 (0.1 M KNO_3 , 25 °C) and comparison with those of related ligands.

<i>h</i>	H_2L1	H_4L2	$H_4te2p^{[25]}$	$H_4te2p-Me_2^{[25]}$	cyclam ^[47]	tmc ^[47]	$H_4teta^{[45]}$
1	10.32	11.43	–	11.47	11.4	9.36	10.7
2	9.87	11.42	26.41 ^[b]	12.17	10.28	9.02	10.13
3	3.44	7.46	6.78	7.20	1.6	2.54	4.10
4	–	6.25	5.36	6.33	2.1	2.25	3.27
5	–	3.61	1.15	1.52	–	–	–
6	–	1.32	–	–	–	–	–

[a] $K_h = [H_hL]/([H] \cdot [H_{h-1}L])$. [b] Overall value for association of two protons.

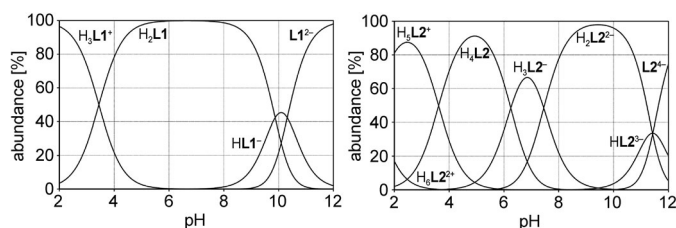


Figure 1. Distribution diagrams of H_2L1 (left) and H_4L2 (right); $c_1 = 0.004$ M.

lead to a reverse order of consecutive protonation constants.^[35] The first deprotonation of H_2L species stabilised by intramolecular hydrogen bonds opens the locked macrocycle conformation, and the second deprotonation proceeds much more easily due to the greater flexibility of the HL species. This leads to a decrease in the solution abundance of the HL species and consequently to a change in the formal order of the corresponding protonation constants if the maximal abundance of the HL species is just one-third or lower, as is graphically shown in Figure S4 of the Supporting Information. If the maximal abundance of the HL species is lower than 33.33%, the abundance curves of the H_2L/HL pair cross each other at a pH ($\log K_2$ value) higher than that of the crossing point of the abundance curves of the HL/L pair ($\log K_1$ value). This results in the order $\log K_a(HL) < \log K_a(H_2L)$. For H_4L2 , this phenomenon (Figure 1) leads to very close values of the first two consecutive protonation constants. The overall basicity over these two steps $\log \beta_2$ (Supporting Information, Table S1) is lower for the phosphinate ligand H_2L1 (20.19) compared to the phosphonate ligand H_4L2 (22.85) as well as to acetate ligands (e.g., H_4teta , 20.83)^[45] due to the electron-withdrawing character of the phosphinate moieties.^[46] Comparing bis(methylphosphonate) ligands, the basicity of the ring amino groups of H_4L2 is slightly lower than that of H_4te2p ($\log \beta_2 = 23.64$)^[25] due to the presence of an electron-withdrawing benzyl group. However, amine basicity of these two phosphonate derivatives with tertiary amino groups is much lower than that of H_4te2p ($\log \beta_2 = 26.41$)^[25] with generally more basic secondary amino groups, similar to difference between cyclam ($\log \beta_2 = 21.68$)^[47] and its N,N',N'',N''' -tetramethyl derivative tmc ($\log \beta_2 = 18.38$)^[47]

Two further protonations of the phosphonate ligand occur on the phosphonate moieties, and the corresponding $\log K_h$ values for formation of H_3L2^- and H_4L2 are 7.46 and 6.25, respectively; these values conform with those reported for analo-

gous processes in related compounds.^[46] Further protonation of H_4L2 occurs on a distant aromatic amino group ($\log K_5(H_5L2^+) = 3.61$) and corresponds well with the analogous process on the phosphinate ligand ($\log K_3(H_3L1^+) = 3.44$). The last protonation constant found for the phosphonate ligand ($\log K_6(H_6L2^{2+}) = 1.32$) describes protonation of some of remaining amino groups of the macrocycle. Further protonation constants were not determined, because they are not accessible by potentiometry. The assignment of protonation sites described above and values of the protonation constants were fully confirmed by the dependence of 1H and ^{31}P NMR shifts on pH (Supporting Information, Figure S5 and Table S1). Some minor discrepancies between the protonation constants obtained by NMR spectroscopy and potentiometry (Supporting Information, Table S1) can be attributed to less precise calibration of the small combined glass electrode used in the NMR experiment (an electrode for direct pH measurement in NMR tubes was used, and it was calibrated by a standard three-point calibration with pH 4, 7 and 10 buffers) and uncontrolled ionic strength in the NMR experiments.

To reach full equilibrium in the M^{II} -ligand mixtures, the systems were studied by an out-of-cell method. The mixtures were equilibrated for 5 d (Cu, Zn) or six weeks (Ni). Stability constants of complexes of the title ligands are compiled in Table 2 and Table S2 of the Supporting Information, and corre-

Table 2. Stability constants $\log K(LM)^{[a]}$ and the corresponding stepwise protonation constants $\log K_{h11}^{[a]}$ of H_2L1 and H_4L2 complexes with selected metal ions (0.1 M KNO_3 , 25 °C).

Constant	H_2L1			H_4L2		
	Ni^{II}	Cu^{II}	Zn^{II}	Ni^{II}	Cu^{II}	Zn^{II}
$\log K(LM)$	11.09	18.25	11.02	16.09	23.29	16.26
$\log K_{111}(HLM)$	5.4	3.87	5.48	7.62	6.90	7.35
$\log K_{211}(H_2LM)$	–	–	–	5.0	5.14	5.20
$\log K_{311}(H_3LM)$	–	–	–	6.1	3.95	5.05

[a] $K_{h11} = [H_hLM]/([H] \cdot [H_{h-1}LM])$.

sponding distribution diagrams are shown in Figure 2. The highest stability was found for Cu^{II} complexes, in accordance with the general Irving–Williams trend. Both ligands show very high selectivity for Cu^{II} ions, as can be seen from a comparison of stability constants of Cu^{II} complexes with those of Ni^{II} and Zn^{II} complexes; the differences are greater than seven orders of magnitude. For a given ligand, stabilities of the Ni^{II} and Zn^{II} complexes are very similar.

For the H_2L1 complexes, the protonation constant of the $[M(HL1)]^+$ species is comparable to $\log K_3$ of the aromatic amino group of the free ligand only for the Cu^{II} complex. For the Ni^{II} and Zn^{II} complexes, these $\log K_{111}$ values are higher by about two orders of magnitude. Thus, one can suggest that equilibrium between deprotonated and monoprotonated species in the $Ni^{II}/Zn^{II}-H_2L1$ systems includes not only protonation of the distant primary aromatic amino group, but also partial protonation of ring amino groups; otherwise, there would be no reason for such high $\log K_{111}$ values of the $[M(HL1)]^+$ species. Therefore, full “in-cage” complexation (i.e., binding by

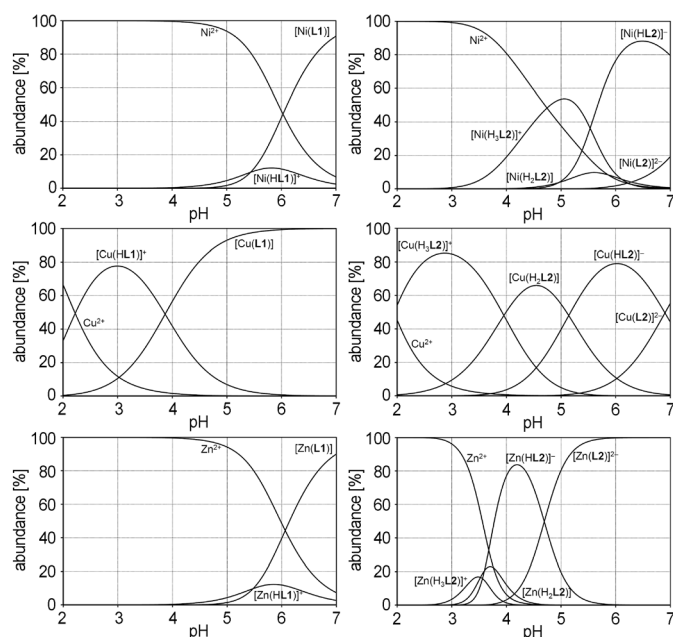


Figure 2. Distribution diagrams of metal-containing species in the M^{II} - H_2L1 (left) and M^{II} - H_4L2 (right) systems; $c_L = c_M = 0.004$ M; $M = Ni$ (top), Cu (middle) and Zn (bottom).

all nitrogen atoms of the macrocycle) in protonated species at acidic pH is suggested only for the $[Cu(HL1)]^+$ complex.

For complexes of the phosphonate ligand H_4L2 , the first two protonations of the complexes should take place on phosphonate groups.^[26,34,35] The resulting doubly protonated species are very probably “in-cage” complexes for all three metal ions (a PO_3H^- group can be firmly bound to central metal ions),^[26,30,35] as almost all corresponding $\log K_f$ values (5.0–7.6, Table 2) are lower than the analogous ones found for the free ligand (7.46 and 6.25, Table 1). Such a decrease is attributable to the electron-withdrawing effect of the coordinated metal ion and it indirectly confirms the expected coordination of a phosphonate pendant arm. Similarly to the phosphinate ligand (see above), the next protonation of the complex species probably occurs fully on the distant aromatic amino group only for the Cu^{II} complex. Further protonation of $[M(H_2L2)]$ to $[M(H_3L2)]^+$ is significantly easier for the Ni^{II} and Zn^{II} complexes and, compared to the analogous protonation of the free ligand, it points again to partial protonation of the amino groups of the macrocycle in these complexes, similar to that suggested above for H_2L1 .

The high complexation selectivity for Cu^{II} over Ni^{II} and Zn^{II} can be clearly seen from distribution diagrams of the M^{II} - H_2L1 / H_4L2 systems (Figure 2) and from summary complexation diagrams shown in Figure S6 of the Supporting Information. Full “in-cage” complexation of Cu^{II} is complete at a pH value of about 4, whereas complexations of Ni^{II} and Zn^{II} start at this pH and are complete at a pH value of about 7 (H_4L2) or even higher (H_2L1).

The stability constants of the M^{II} - H_2L1 / H_4L2 complexes are compared with those of complexes of related ligands in Table 3. However, values of stability constants alone are not

Table 3. Comparison of stability constants of complexes of M^{II} with H_2L1 , H_4L2 and related ligands.

Ligand	$\log \beta_{NiL}$	$\log \beta_{CuL}$	$\log \beta_{ZnL}$	$pCu^{[a]}$
H_2L1	11.09	18.25	11.02	7.63
H_2L2	16.09	23.29	16.26	8.71
$H_2te2p^{ABn[48]}$	–	23.94 (pc) ^[b] (trans) ^[c]	24.08	17.16 8.94 (pc) ^[b] (trans) ^[c]
H_4te2p	21.99 ^[32]	25.40 (pc) ^[b] (trans) ^[c,26]	26.50	20.35 ^[32] 8.13 (pc) ^[b] (trans) ^[c]
H_4te2p - $Me_2^{[35]}$	15.55	24.03 (pc) ^[b]	17.56	8.74 (pc) ^[b]
cyclam ^[47]	22.2	28.1	15.2	11.81
tmc ^[47]	8.65	18.3	10.4	8.55
$H_4teta^{[47]}$	20.00	21.74	16.62	9.03

[a] pCu is the negative logarithm of free Cu^{II} concentration in solution ($c_{Cu} = c_L = 0.004$ M, pH 7.4). [b] pc = pentacoordinate kinetic isomer. [c] trans = trans-*O,O'* octahedral thermodynamic isomer.

sufficient to compare the stabilities of the complexes,^[46] because the ligands also differ significantly in proton affinity, and metal-ion complexation and protonation are concurrent processes. Therefore, the $-\log[Cu^{II}] = pCu$ parameter was also calculated under the conditions used in potentiometry ($c_{Cu} = c_L = 0.004$ M) and at physiological pH 7.4. The stabilities of the Cu^{II} complexes of the novel ligands are comparable/only slightly lower than those of other cyclam derivatives but still sufficient for possible in vivo radiocopper applications. The observed high selectivity for divalent copper can be employed in the removal of copper from mixtures of metal ions, for example, in separation/purification of radiocopper (see below).

Formation kinetics of the copper(II) complexes

Since the complexation rate is a central point for possible radiochemical applications, formation kinetics of copper(II) complexes was studied in detail. Formation of copper(II) complexes of the title ligands was monitored directly by UV/Vis spectroscopy in the pH range 2.4–7.2 (chloroacetate, acetate, phosphate and 2-(*N*-morpholino)ethanesulfonic acid (MES) buffers). At $pH < 4.5$, conventional measurements were employed. At $pH > 4.5$, the stopped-flow technique was used, since the complexation reactions were very fast. The formation kinetics correspond to a first-order process with respect to Cu^{II} , as the dependence of $f_{k_{obs}}$ on Cu^{II} concentration at constant pH is linear (Supporting Information, Figure S7). A negligible role of the coordinating anions in acetate or phosphate buffers on the complexation process was confirmed by the independence of $f_{k_{obs}}$ from buffer concentration at constant pH (Supporting Information, Figure S8). When acetate and phosphate buffers were used at similar pH values, the experiments gave similar results with expected trends and showed no difference between both buffers (Supporting Information, Figure S8). Coordination ability of chloroacetate and MES buffers was also expected to be negligible.^[49] The complexation reactions were monitored under pseudo-first-order conditions with a large excess of Cu^{II} ions, and the observed rate constants were divided by Cu^{II} concentration to obtain second-order rate constants

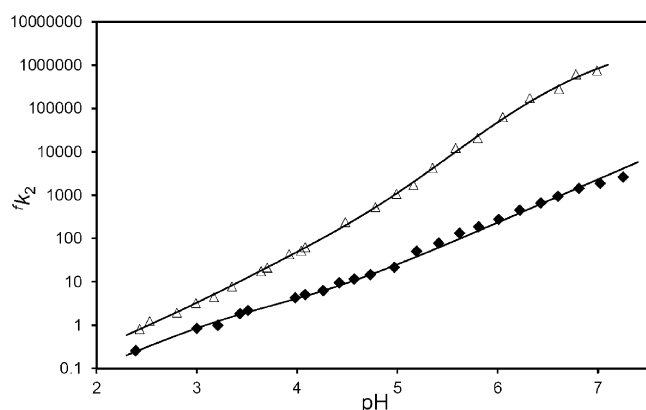


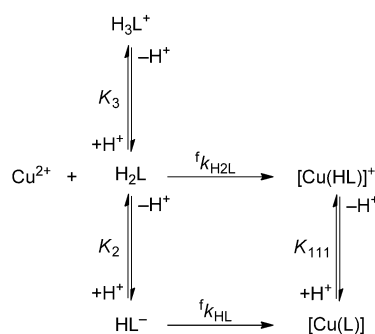
Figure 3. pH dependence of second-order rate constant f_k2 for complexation reactions in the $\text{Cu}^{\text{II}}\text{-H}_2\text{L1}$ (full diamonds) and $\text{Cu}^{\text{II}}\text{-H}_4\text{L2}$ (empty triangles) systems ($t = 25.0^\circ\text{C}$, $l = 0.1\text{ M KCl}$). Lines represent the best fits to Equation (1) for the $\text{Cu}^{\text{II}}\text{-H}_2\text{L1}$ system and Equation (2) for the $\text{Cu}^{\text{II}}\text{-H}_4\text{L2}$ system with values from Table 4.

f_k2 . The f_k2 values are compiled in Tables S3 and S4 of the Supporting Information and shown in Figure 3. The overlay of the pH dependence of f_k2 and the distribution diagrams of the free ligands (Supporting Information, Figure S9) clearly shows that several differently protonated species must be taken into account for treatment of the formation kinetics data. For the $\text{Cu}^{\text{II}}\text{-H}_2\text{L1}$ system, the HL1^- species must be included in the fitting (although its abundance is negligible in the studied pH range), since f_k2 is still increasing with pH even in the pH range 5.5–7, in which the ligand is present to approximately 100% as the zwitterionic $\text{H}_2\text{L1}$ form. Therefore, the data were fitted by testing different combinations of reacting species, with ligand protonation constants fixed to the values found by potentiometry (Table 1). The best results were obtained by using Equations (1) and (2) for the $\text{Cu}^{\text{II}}\text{-H}_2\text{L1}$ and $\text{Cu}^{\text{II}}\text{-H}_4\text{L2}$ systems, respectively, where K_n are stepwise protonation constants of the free ligands and species reactivities are characterised by $f_k(\text{H}_n\text{L})$ constants. It corresponds to reaction mechanisms shown in Schemes 3 and 4, and contributions of individual species to the overall reactivity are shown in Figures S10 and S11 of the Supporting Information. Rate constants $f_k(\text{H}_n\text{L})$ corresponding to differently protonated ligand species are listed in Table 4.

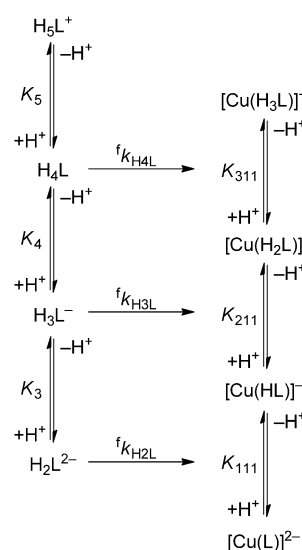
$$f_k2 = \frac{f_k(\text{HL}) + f_k(\text{H}_2\text{L}) \cdot K_2 \cdot [\text{H}^+]}{K_2 \cdot [\text{H}^+] + K_2 \cdot K_3 \cdot [\text{H}^+]^2} \quad (1)$$

$$f_k2 = \frac{f_k(\text{H}_2\text{L}) + f_k(\text{H}_3\text{L}) \cdot K_3 \cdot [\text{H}^+] + f_k(\text{H}_4\text{L}) \cdot K_3 \cdot K_4 \cdot [\text{H}^+]^2}{1 + K_3 \cdot [\text{H}^+] + K_3 \cdot K_4 \cdot [\text{H}^+]^2 + K_3 \cdot K_4 \cdot K_5 \cdot [\text{H}^+]^3} \quad (2)$$

Figure 3 shows that phosphonate ligand $\text{H}_4\text{L2}$ binds copper(II) faster than phosphinate ligand $\text{H}_2\text{L1}$ by 1–2 order(s) of magnitude, with increasing difference on going to higher pH. Compared to other related systems reported in the literature, the overall reaction rate of the phosphonate ligand $\text{H}_4\text{L2}$ is



Scheme 3. Proposed mechanism of complexation of the $\text{Cu}^{\text{II}}\text{-H}_2\text{L1}$ system.



Scheme 4. Proposed mechanism of complexation of the $\text{Cu}^{\text{II}}\text{-H}_4\text{L2}$ system.

Rate constant	$\text{H}_2\text{L1}$	$\text{H}_4\text{L2}$	$\text{H}_4\text{te2p}^{[26]}$	$\text{H}_4\text{te2p-Me}_2^{[35]}$	cyclam	tmc ^[51]
	[s ⁻¹ mol ⁻¹ dm ³]					
$f_k(\text{HL})$	$1.72(9) \times 10^6$	–	–	–	1.05×10^6 , ^[52] 1.8×10^6 , ^[53] 8.0×10^6 , ^[54]	2.9×10^5
$f_k(\text{H}_2\text{L})$	2.98(16)	$3.66(17) \times 10^6$	1.97×10^5	2.8×10^6	0.135, ^[52] 0.39, ^[53] 0.076 ^[54]	–
$f_k(\text{H}_3\text{L})$	–	$9.1(7) \times 10^3$	1.38×10^3	2.8×10^3	–	–
$f_k(\text{H}_4\text{L})$	–	11.7(9)	0.17	0.04	–	–

comparable to those of other ligands with two phosphonate pendant arms ($\text{H}_4\text{te2p}^{[26]}$ and parent $\text{H}_4\text{te2p-Me}_2^{[35]}$ Supporting Information, Figure S12). The complexation proceeds via analogous protonated species with similar reactivities of the individual species (Table 4). In contrast, the reactivity of phosphinate ligand $\text{H}_2\text{L1}$ is similar (Supporting Information, Figure S12) to that of *N*-benzylcyclam and, based on data published previous-

ly, to those of tmc^[51] and cyclam itself^[52–54] (for formulae, see Scheme 1). *N*-Benzylcyclam was chosen as a simple model derivative for comparison; it emulates our bifunctional derivatives by having a related side group but no coordinating pendant arms.

Efficiency of copper(II) incorporation by these ligands was also tested radiochemically at pH 5.5. ⁶⁴Cu labelling is faster in comparison to the UV/Vis experiments, and this is caused by a large excess of the ligands over ⁶⁴Cu^{II}.^[50] The phosphonate ligand H₄L₂ forms ⁶⁴Cu^{II} complexes at ambient temperature very rapidly (radiochemical yield >95% within 10 min). Similar results were obtained for cyclam and *N*-benzylcyclam. However, under these conditions, complexation with the phosphinate ligand H₂L₁ requires a longer time; only about 60% of H₂L₁ is labelled with ⁶⁴Cu after 10 min. Full complexation requires 90 min at ambient temperature. However, the labelling efficacy of this ligand was significantly increased at higher temperature. Almost quantitative ⁶⁴Cu labelling of H₂L₁ was observed at 50 °C within 10 min.

For ligand H₄L₂, in the studied pH range, the most reactive species is doubly protonated H₂L₂²⁺, in which both protons are bound to the nitrogen atoms of the macrocycle (see above) and the phosphonate pendant arms are fully deprotonated. The reactivity of this species fully governs the overall rate of complex formation above a pH value of about 5 (Supporting Information, Figure S11). On protonation of the phosphonate moieties affording H₃L₂⁺ and H₄L₂, the reactivity gradually decreases and, for the neutral zwitterionic H₄L₂, is similar to that of the analogous zwitterionic form of phosphinate ligand H₂L₁ (i.e., doubly protonated macrocycle with each of pendant arms bearing a charge of 1–; see Table 4). Contrary to phosphonate ligand H₄L₂, the most reactive species of phosphinate ligand H₂L₁ in the studied pH range is HL₁[–], which drives the overall reaction above about pH 4.5 (Supporting Information, Figure S10). The monoprotonated species is generated much more easily for H₂L₁ than for H₄L₂ due to the significantly lower log *K*₂ value of the ring amino group (9.87 vs. 11.42, respectively; Table 1) and uncharged nature of H₂L₁. Therefore, HL₁[–] can significantly contribute to the overall complexation rate even in the slightly acidic region. The corresponding rate constant *k*(HL) is somewhat higher than that reported for tmc and is comparable to that of cyclam itself (Table 4).

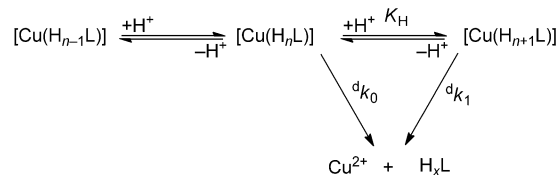
The results clearly show that the nature of pendant arms is decisive for the rate of formation of copper(II) complexes of the macrocyclic ligands. The highest overall reaction rate was observed for ligands containing phosphonate group(s), which have higher complexation ability than phosphinate group(s). Considering the general mechanism of complex formation by macrocycle ligands, whereby formation of weak “out-of-cage” complexes proceeds the final “in-cage” coordination, a higher abundance of the “out-of-cage” species should accelerate overall complex formation. Therefore, stronger affinity of the phosphonates to metal ions should lead to a more abundant “out-of-cage” complex and to an increase in effective copper(II) concentration in the vicinity of the macrocyclic unit; this accelerates the rate-determining “in-cage” binding. Weakly coordinating pendant groups such as *N*-methylphosphinates

do not affect the reaction significantly compared with the simple ligands. This supports reports made on complexation of NCA ⁶⁴Cu with phosphonate-containing cross-bridged cyclam derivatives claiming fast and quantitative ⁶⁴Cu binding even at room temperature.^[55] Anyway, reactivity of the monoprotonated species points to the fact that the presence of weakly coordinating phosphinate pendant arms somewhat accelerates “in-cage” complex formation with H₂L₁ compared to that with tmc; however, if the different ligand basicities are taken into account, the overall reactivities of the two ligands are similar (Supporting Information, Figure S12).

Dissociation kinetics of the copper(II) complexes

The acid-assisted dissociation of copper(II) complexes of H₂L₁ and H₄L₂ was investigated in 0.025–4.89 M HClO₄ and (H₂Na)ClO₄ with an ionic strength of 5.0 M at room and elevated temperatures. The experimentally observed ^d*k*_{obs} values are compiled in Tables S5 and S6 of the Supporting Information. The data of complexes of both ligands were successfully fitted by Equation (3) corresponding to the mechanism shown in Scheme 5. The results are listed in Table 5, and the best fits are shown in Figure 4.

$${}^d k_{\text{obs}} = \frac{{}^d k_0 + {}^d k_1 \cdot K_{\text{H}} \cdot [\text{H}^+]}{1 + K_{\text{H}} \cdot [\text{H}^+]} \quad (3)$$



Scheme 5. Proposed mechanism of acid-assisted dissociation Cu^{II}–H₂L₁ and Cu^{II}–H₄L₂ complexes.

The number of protons in kinetically active species is obviously different in the two complexes (Scheme 5) due to the protonatable phosphonate groups in H₄L₂. According to distribution diagrams (Figure 2), protonation of the distant amino group of the aminobenzyl unit is expected for systems with both ligands, and thus probably mono- (*n* = 1, ^d*k*₀) and diprotonated (^d*k*₁) species are kinetically important for the Cu^{II}–H₂L₁ complex, and tri- (*n* = 3, ^d*k*₀) and tetraprotonated (^d*k*₁) are kinetically decisive for the Cu^{II}–H₄L₂ complex. Although a simplified equation with ^d*k*₀ = 0 is commonly sufficient for good fit of experimental data (e.g., as was used for the Cu^{II}–H₄te2p-Me₂ complex),^[35] inclusion of this particular rate constant significantly improved fits by lowering the observed sum of squared deviations by 20–30%. However, this rate constant was calculated with relatively large uncertainty (Table 5).

The dissociation rates and their temperature dependences are very similar for both studied systems. Activation parameters (obtained from linearisations shown in Supporting Information, Figures S13–S15) of the proton-assisted dissociation

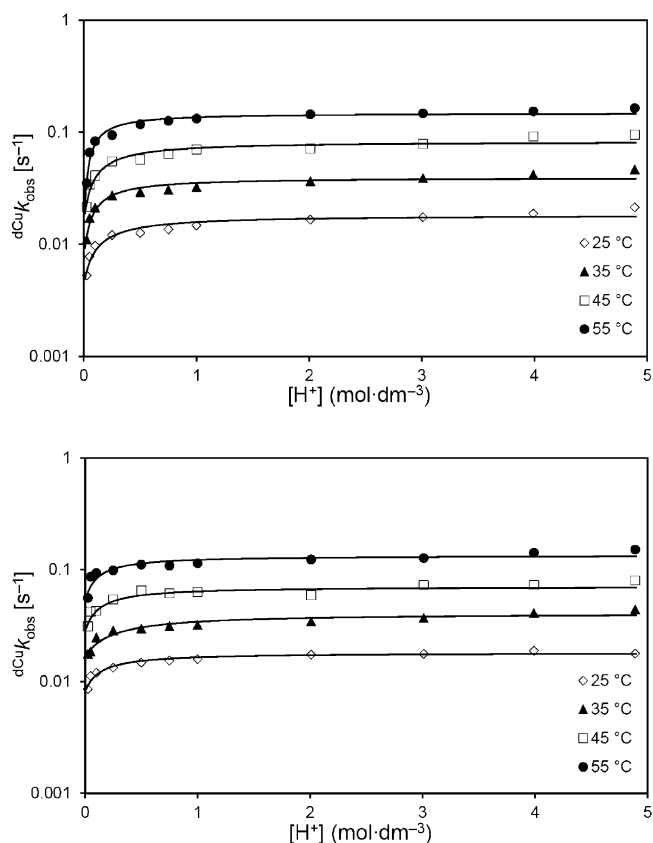


Figure 4. Dependence of $d_{\text{Cu}}/k_{\text{obs}}$ for acid-assisted decomplexation of $\text{Cu}^{\text{II}}\text{-H}_2\text{L1}$ (top) and $\text{Cu}^{\text{II}}\text{-H}_4\text{L2}$ (bottom) complexes at $T=25, 35, 45$ and $55\text{ }^\circ\text{C}$ (empty diamonds, full triangles, empty squares and full circles, respectively); $I=5.0\text{ M}$ $(\text{H,Na})\text{ClO}_4$. Lines represent the best fits to Equation (3) for values from Table 5.

step (characterised by $^d k_1$) are comparable with those reported for the $\text{Cu}^{\text{II}}\text{-H}_4\text{te2p-Me}_2$ complex^[35] and indicate the same decomplexation mechanism. The values of the protonation constants describing the equilibrium between the dissociating species ($\log K_{\text{H}} = \text{p}K_{\text{A}} \approx 0.7\text{--}0.8$, Table 5) indicate initial protonation of the phosphorus acid moiety. Such values also support the estimated number of protons in the reactive species (see above). Both studied complexes exhibit lower inertness towards acid-assisted decomplexation than the $\text{Cu}^{\text{II}}\text{-H}_4\text{te2p-Me}_2$ complex^[35] and much lower inertness than those of the ligands with secondary amino groups.^[26,48] Decomplexation half-lives of complexes of the title ligands are compared with those of complexes of selected related ligands in Table 6.

The results show that copper(II) complexes of *N*-tetrasubstituted cyclam derivatives are generally much more kinetically labile than complexes of less *N*-substituted cyclam-based ligands with secondary amino groups. Therefore, the title bifunctional ligands may be convenient for applications in which fast decomplexation is required, for example, separation of copper(II) ions (see below).

Synthesis and characterisation of ion-selective resins

The selectivity of the studied ligands towards copper(II) complexation and relatively low kinetic inertness can be potentially employed for separation of copper(II) from mixtures of other metal ions due to its selective complexation. Separation/removal of copper(II) ions from other metal ions is of interest, for example, in the treatment of Wilson's disease (metabolic disorder causing overload of the human body with divalent copper),^[57–61] in the preparation of copper radioisotopes^[62–65]

Rate/equilibrium constants	Temperature [$^\circ\text{C}$]				Activation/thermodynamic parameters
	25	35	45	55	
$\text{Cu}^{\text{II}}\text{-H}_2\text{L1}$					
$^d k_0$ [s^{-1}]	$4.33(95) \times 10^{-3}$	$7.4(2.4) \times 10^{-3}$	$1.55(44) \times 10^{-2}$	$1.0(1.0) \times 10^{-2}$	$E_a = 29.2(13.0)\text{ kJ mol}^{-1[\text{a}]}$ $\Delta H^\ddagger = 26.6(13.0)\text{ kJ mol}^{-1[\text{b}]}$ $\Delta S^\ddagger = -200(42)\text{ JK}^{-1}\text{ mol}^{-1[\text{b}]}$
$^d k_1$ [s^{-1}]	$1.83(12) \times 10^{-2}$	$3.95(22) \times 10^{-2}$	$8.29(51) \times 10^{-2}$	$1.48(7) \times 10^{-1}$	$E_a = 57.1(1.5)\text{ kJ mol}^{-1[\text{a}]}$ $\Delta H^\ddagger = 54.5(1.5)\text{ kJ mol}^{-1[\text{b}]}$ $\Delta S^\ddagger = -95(5)\text{ JK}^{-1}\text{ mol}^{-1[\text{b}]}$
K_{H} [$\text{mol}^{-1}\text{ dm}^3$]	4.6(2.0)	6.5(2.6)	5.3(2.1)	9.9(3.4)	$\Delta H = 16.9(8.8)\text{ kJ mol}^{-1[\text{c}]}$ $\Delta S = 69(28)\text{ JK}^{-1}\text{ mol}^{-1[\text{c}]}$
$\log K_{\text{H}}$	0.66	0.81	0.72	1.00	
$\text{Cu}^{\text{II}}\text{-H}_4\text{L2}$					
$^d k_0$ [s^{-1}]	$8.03(77) \times 10^{-3}$	$1.65(12) \times 10^{-2}$	$2.76(52) \times 10^{-2}$	$5.15(97) \times 10^{-2}$	$E_a = 49.6(1.8)\text{ kJ mol}^{-1[\text{a}]}$ $\Delta H^\ddagger = 47.0(1.8)\text{ kJ mol}^{-1[\text{b}]}$ $\Delta S^\ddagger = -127(6)\text{ JK}^{-1}\text{ mol}^{-1[\text{b}]}$
$^d k_1$ [s^{-1}]	$1.81(6) \times 10^{-2}$	$4.08(18) \times 10^{-2}$	$7.07(42) \times 10^{-2}$	$1.34(6) \times 10^{-1}$	$E_a = 53.4(2.3)\text{ kJ mol}^{-1[\text{a}]}$ $\Delta H^\ddagger = 50.8(2.3)\text{ kJ mol}^{-1[\text{b}]}$ $\Delta S^\ddagger = -108(7)\text{ JK}^{-1}\text{ mol}^{-1[\text{b}]}$
K_{H} [$\text{mol}^{-1}\text{ dm}^3$]	5.1(1.9)	2.68(87)	5.3(3.2)	6.1(3.1)	$\Delta H = 9.5(14.9)\text{ kJ mol}^{-1[\text{c}]}$ $\Delta S = 43(48)\text{ JK}^{-1}\text{ mol}^{-1[\text{c}]}$
$\log K_{\text{H}}$	0.71	0.43	0.72	0.79	

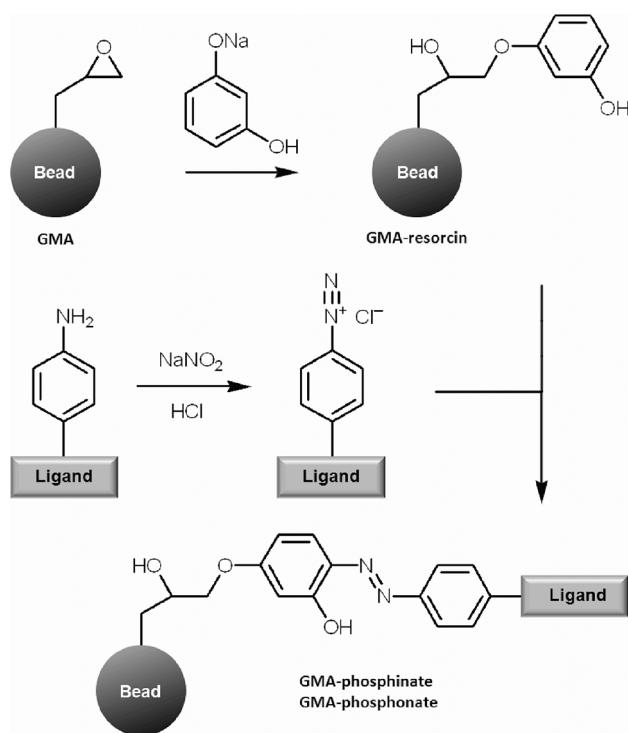
[a] Arrhenius model: $[\ln k = -(E_a/RT) + \ln A]$. [b] Eyring model: $[\ln(k/T) = -(\Delta H^\ddagger/RT) + (\Delta S^\ddagger/R) + \ln(k_b/h)]$. [c] $\ln K_{\text{H}} = -(\Delta H/RT) + (\Delta S/R)$.

Ligand	$\tau_{1/2}$
H ₂ L1	44 s
H ₄ L2	42 s
H ₄ te2p-Me ₂ ^[35]	2.5 min
<i>N</i> -benzylcyclam	9.1 min
H ₄ te2p (pc) ^[5] ^[26]	19.7 min
cyclam ^[56]	20.9 min

[a] pc = pentacoordinated kinetic isomer.

and in technological applications (e.g., removal of copper(II)/other ions from wastewater).^[66–74]

To test our ligands in radiocopper purification, the ligands were covalently immobilised on hydrophilic, macroporous polymer beads (Scheme 6). The rate of adsorption of metal ions on polymer beads generally depends on the rate of complexation by immobilised ligands and on transport phenomena, especially on the diffusion rate and the accessibility of the chelating groups. Thus, macroporous hydrophilic beads were chosen, because they ensure both rapid diffusion and good accessibility of the complexing groups. If a rapidly complexing chelator is covalently attached to a macroporous matrix, uptake of metal ions from aqueous solution typically proceeds within a few minutes in a batch experiment.^[58] We chose poly(glycidyl methacrylate-*co*-ethylene dimethacrylate) (GMA) beads as a starting material^[75] containing reactive epoxide groups that are suitable for further synthetic transformations.



Scheme 6. Schematic representation of modification of macroporous polymer beads by ligands H₂L1 and H₄L2.

They were treated with the monosodium salt of resorcinol in analogy to the reaction with pheno^[76] to afford polymer-immobilised 1-hydroxy-3-alkoxybenzene moieties as highly activated, passive azo coupling components (Scheme 6). Sodium resorcinolate was used instead of resorcinol to increase the nucleophilicity and facilitate reaction with the polymeric epoxides. Successful reaction was confirmed by solid-state ¹³C{¹H} NMR spectra, in which aromatic carbon signals of the product were found to be equivalent to the resorcinol content of 0.974 mmol g⁻¹.

The polymer-immobilised resorcinol was further used as a passive azo coupling component for diazotised macrocyclic ligands. This synthetic strategy was modified from previously published immobilisation of chelating agents on soluble polymers containing phenolic moieties.^[77] The progress of the reaction was obvious due to the development of an intense orange colour caused by formation of azo-group chromophores; it was confirmed by IR spectroscopy and ³¹P{¹H} solid-state NMR spectroscopy. The IR spectrum showed significant increase in OH signal intensity at 3100–3600 cm⁻¹, corresponding to successful loading of OH-rich macrocyclic ligands (Supporting Information, Figure S16). Other signals typical for the ligand (P=O etc.) could not be detected due to overlap with GMA-resorcinol signals in the region 500–1500 cm⁻¹. The change in the ¹³C{¹H} solid-state NMR spectra was not significant; however, the ³¹P{¹H} solid-state NMR spectrum clearly showed the appearance of broad signals centred at 21 and 18 ppm for resin-H₂L1 and resin-H₄L2 product materials, respectively. Ligand contents in the polymers, determined by copper(II) chelation capacity, were 65 and 44 μmol g⁻¹ for resin-H₂L1 and resin-H₄L2, respectively, which are sufficient for the intended use in radionuclide separation.

The advantage of this simple two-step immobilisation is visibility of the reaction progress (formation of orange azo dye, Scheme 6) as well as a lack of charged components except the ligands themselves on the bead surface in the relevant pH range, so that the beads do not behave as a non-selective electrostatic ion exchanger. Other coupling conditions were also tested. Direct reaction of the aromatic primary amino groups of the bifunctional ligand with epoxide groups gave an unsatisfactory yield, whereas aminolysis of a chlorosulfonated polymer support with the aromatic primary amino groups of the ligand left many free sulfo groups (formed after complete hydrolysis of the polymers), and thus the final product behaved as a non-selective strong cation exchanger rather than a selective chelating resin.

The azo-dye-loaded macrocyclic ligands were tested for sorption of trace amounts of copper(II) in the presence of large excess of zinc(II) and nickel(II) ions (ca. 400–500 molar excess), which is a model for the intended application, that is workup of cyclotron targets for radiocopper production by separating trace amounts of radiocopper from irradiated nickel/zinc targets. As nickel(II)/zinc(II) concentrations, typical values obtained after dissolution of cyclotron-irradiated target discs were chosen (≈ 10 mg cm⁻³), and c(Cu^{II}) was about 0.02 mg cm⁻³ to ensure a reasonable sensitivity of detection by atomic absorption spectroscopy (AAS). The copper concentra-

Table 7. Relative concentrations ($c(M^{2+})$ in % of the original amount) of metal ions found in supernatants after metal loading, washing and acid-assisted desorption. The nickel(II)/zinc(II) concentrations in the primary loading solution were about 10 mg cm^{-3} , and the copper(II) concentration in primary loading solution was about 0.02 mg cm^{-3} .

Supernatant/parameter of sorption	pH 3				pH 5			
	Cu/Ni binding		Cu/Zn binding		Cu/Ni binding		Cu/Zn binding	
	$c(\text{Cu})$	$c(\text{Ni})$	$c(\text{Cu})$	$c(\text{Zn})$	$c(\text{Cu})$	$c(\text{Ni})$	$c(\text{Cu})$	$c(\text{Zn})$
resin-H ₂ L1								
supernatant after metal loading	67.0	93.3	72.5	95.3	4.7	91.1	4.3	93.9
washing, 1st cycle	5.2	6.4	4.2	4.4	6.9	8.3	7.9	5.7
washing, 2nd cycle	3.0	0.3	2.7	0.3	7.1	0.5	6.9	0.4
desorption, 1st cycle	22.2	0.0	18.4	0.0	72.4	0.0	72.3	0.0
desorption, 2nd cycle	2.6	0.0	2.2	0.0	8.9	0.0	8.6	0.0
total bound metal	24.8	0	20.6	0	81.3	0	80.9	0
selectivity coefficient Cu/M ^[a]	1.7×10^3		1.2×10^3		4.4×10^4		5.4×10^4	
resin-H ₄ L2								
supernatant after metal loading	57.8	91.8	63.6	94.6	6.8	98.2	6.3	93.6
washing, 1st cycle	5.3	7.7	4.9	5.1	7.7	1.2	9.9	6.0
washing, 2nd cycle	3.8	0.5	3.5	0.3	7.8	0.5	8.2	0.4
desorption, 1st cycle	29.8	0.0	25.6	0.0	68.5	0.0	55.3	0.0
desorption, 2nd cycle	3.4	0.0	2.4	0.0	9.1	0.0	20.3	0.0
total bound metal	33.2	0	28.0	0	77.6	0	75.6	0.0
selectivity coefficient Cu/M ^[a]	1.9×10^3		1.8×10^3		3.2×10^4		4.7×10^4	

[a] Selectivity coefficient is defined as $\{[Cu^{2+}]_{\text{adsorbed}}/[Cu^{2+}]_{\text{solution}}\}/\{[M^{2+}]_{\text{adsorbed}}/[M^{2+}]_{\text{solution}}\}$.

tion was kept as low as possible to mimic cyclotron target workup, in which radiocopper is present only in traces. The molar amount of metal-binding sites of the complexing resin was about twice the total amount of copper(II) in solution. Two solution acidities were chosen (pH 3.0 and 5.0). At the lower pH, copper(II) should be almost completely complexed according to the distribution diagrams, whereas the other metal ions should not be bound at all, and at the higher pH Ni^{II} and Zn^{II} ions start to be bound by the title ligands (Figure 2). Weakly chelating chloroacetate (pH 3) and acetate (pH 5) buffers were chosen to prevent hydrolysis and/or precipitation of metal hydroxides, especially at pH 5.0. The metal salts were 1) adsorbed by the resin in the buffered solution, 2) the excess of the solution was washed out by washing with pH 3.0 buffer (two washings, to remove any non-specifically bound metal ions) and 3) metal ions were desorbed from the resin with 1 M aqueous hydrochloric acid (two portions). In each supernatant, the metal content was determined by AAS. An overview of the analytical data is given in Table S7 of the Supporting Information, and the results are listed in Table 7.

In all cases, only trace amounts of nickel or zinc were adsorbed on the sorbents at both pH 3.0 and 5.0 (concentrations were at the detection limit of the analytical method used; see Supporting Information, Table S7). The two modified resins gave similar results: at pH 3.0, copper(II) is adsorbed only partly (20–30%), but at pH 5, about 80% of copper(II) is adsorbed. Copper desorption by hydrochloric acid was found to be nearly quantitative (from copper balance); this is a prerequisite for reuse of the sorbent. On going from pH 3.0 to 5.0, the selectivity coefficients increase by more than one order of magnitude. Thus, a pH of about 5 seems to be ideal for the most selective binding of divalent copper (and copper radio-

isotopes) by these ligands. Such a pH is commonly used for labelling of biomolecules with copper radioisotopes. Thus, this finding may also be exploitable for selective labelling of radiopharmaceuticals, in which impurities in solutions of copper radionuclides disturb the labelling process.

Separation of ⁶⁴Cu/^{nat}Cu from ^{nat}Ni ions

To further demonstrate possible utilisation of the resins in separating ⁶⁴Cu from non-radioactive divalent metals (Ni^{II} and Zn^{II}), experiments with an NCA [⁶⁴Cu]CuCl₂ solution were carried out. The protocol followed the procedure described above for non-radioactive sorption experiments. The ⁶⁴Cu isotope was produced via the ⁶⁴Ni(p,n)⁶⁴Cu reaction. Separation of ⁶⁴Cu/^{nat}Cu from ⁶⁴Ni utilises the well-known anion-exchange methodology described previously.^[78] To study selectivity of the sorption process, a defined amount of natural Ni^{II} was added to carrier-free [⁶⁴Cu]CuCl₂ solution. Metal sorption was performed at pH 5.5, and the efficiency of sorption and desorption processes was studied by radioactivity measurements (Tables 8 and 9), and was independently determined by inductively coupled plasma mass spectrometry (ICP-MS) after complete decay of the ⁶⁴Cu radioactivity (i.e., the found Cu^{II} concentrations corresponds to traces of the non-radioactive copper present in the starting solutions; Supporting Information, Tables S8 and S9). However, ICP-MS measurements are rather qualitative, as concentrations of metal ions in several cases lay at the edge of detection limit (ppb) of the method.

For adsorption experiments, the solution containing ⁶⁴Cu^{II} and excess of natural Ni^{II} was added to the studied resin and the suspension was incubated for 30 min. After this time, resin was separated from the supernatant and rinsed with buffer so-

Table 8. Balance of ^{64}Cu radioactivity [MBq] (decay-corrected instrument reading) after adsorption of ^{64}Cu on resins.

Material	resin- $\text{H}_2\text{L1}$	resin- $\text{H}_4\text{L2}$
total activity added to resin	51.53	52.18
resin, after adsorption	40.91 (79%)	44.36 (85%)
supernatant, after adsorption	10.54 (21%)	7.75 (15%)
resin, after washing (three times)	33.10 (64%)	37.67 (72%)
washing solutions	7.25	6.38

Table 9. Balance of ^{64}Cu radioactivity [MBq] (decay-corrected instrument reading) after desorption of ^{64}Cu from the studied resins using 1 M aq. HCl.

Material	resin- $\text{H}_2\text{L1}$	resin- $\text{H}_4\text{L2}$
starting activity	33.10	37.67
resin, after 15 min desorption	7.23	7.43
supernatant, after 15 min desorption	25.78 (50%) ^[a]	30.06 (58%) ^[a]
resin, after washing (three times)	1.93	0.60
scrubbing solutions	5.13	6.74
total desorbed activity	30.91 (93%) ^[b]	36.80 (98%) ^[b]

[a] Based on total activity loaded to resin (Table 8). [b] Based on activity retained by resin.

lution (pH 5.5, three times). For desorption experiments, the copper-loaded resin was rinsed once with 1 M aqueous HCl, and after centrifugation, again three times with 1 M aqueous HCl. After each step, radioactivities of resin and scrubbing solutions were measured (Tables 8 and 9).

Balances of ^{64}Cu activities showed retention of about 70% of radioactivity on the resin and nearly quantitative recovery of this amount after repeated washing. In the first washing cycle (1 M aq. HCl), about 50–60% of total starting activity was isolated (Table 9). The two resins behave similarly; however, the phosphonate-based resin- $\text{H}_4\text{L2}$ shows slightly better parameters than phosphinate-containing resin- $\text{H}_2\text{L1}$. In both cases, very good separations of radiocopper from Ni^{II} were achieved: almost all Cu^{II} was adsorbed in the presence of a 900-fold excess of Ni^{II} , and sorption of Ni^{II} was negligible under these conditions (Supporting Information, Tables S8 and S9); this is an important property for the recovery of expensive isotopically pure ^{64}Ni . However, exact quantification of ICP-MS results is problematic due to the very low content of Cu^{II} , close to the detection limit of the method.

Conclusion

Two new bifunctional cyclam-based macrocyclic ligands with two coordinating phosphorus acid pendant arms and *p*-amino-benzyl side group were synthesised by simple approaches employing glyoxal bis-aminal protection of cyclam. The results showed that the title ligands are among the most suitable for selective copper(II) complexation. The copper(II) complexes are thermodynamically stable ($\log\beta_{\text{CuL}} = 18.3$ and 23.3 for $\text{H}_2\text{L1}$ and $\text{H}_4\text{L2}$, respectively) and are formed with a high selectivity over nickel(II) and zinc(II) complexes ($\log\beta_{\text{ML}}$ is ca. 11 for $\text{H}_2\text{L1}$

and ca. 16 for $\text{H}_4\text{L2}$ for each metal ion). Copper(II) ions are quantitatively complexed above a pH of about 3.5 ($c_{\text{L}} = c_{\text{M}}$, millimolar range). Ligand $\text{H}_4\text{L2}$ binds copper(II) ions very fast at a pH of about 5, whereby no significant complexation of zinc(II) and nickel(II) ions occurs; copper(II) complexation by $\text{H}_2\text{L1}$ over Ni^{II} and Zn^{II} is also very selective, but the Cu^{II} complexation rate is about two orders of magnitude slower than that of $\text{H}_4\text{L2}$ and is comparable to that of cyclam and its derivatives without coordinating pendant arms. The copper(II) complexes of both ligands are moderately kinetically inert towards acid-assisted dissociation (half-lives: 44 s ($\text{H}_2\text{L1}$) and 42 s ($\text{H}_4\text{L2}$) in 1 M aq. HClO_4 at 25 °C). However, their decomplexation rates are much higher than those of complexes of other cyclam derivatives and are among the highest described till now. Therefore, the current studies have shown the great potential of *N,N''*-dialkyl-*N,N''*-bis(methylphosphinic/methylphosphonic acid) cyclam derivatives as building blocks of resins for selective copper(II) complexation. This was documented by preparing polymer beads modified by the title ligands through an azo coupling reaction and studying their performance in the separation of copper(II) from other metal ions. After complexation and washing off the other metal ions, the Cu^{II} ion can be released from the resin by elution with a strong acid due to the kinetic lability of the complexes. This concept operates well even at the very low concentrations relevant to working with copper radionuclides, as documented by model separation of NCA ^{64}Cu from large excess of Ni^{II} . This proof-of-concept study shows that proper tuning of ligand and polymer properties can lead to selective resins for purification of copper and, after appropriate modification of the chelator, other metal radionuclides for biological/medical applications.

Experimental Section

General

Cyclam (1,4,8,11-tetraazacyclotetradecane, Chematech), hypophosphorous acid (50% aq. solution, Fluka), triethyl phosphite (Fluka), D_2O (99.95% D, Chemtrade) and Dowex 50 (100–200 mesh, Fluka) were used without further purification. Cyclam formaldehyde **1**^[37] and glyoxal **2**^[33] bis-aminals and monoquaternary salt **3**^[33] were synthesised according to literature methods. *N*-Benzylcyclam was prepared according to the published procedure.^[79] Paraformaldehyde was filtered from an old formaldehyde solution and dried over P_2O_5 in vacuo. NMR spectra were recorded on a Varian S300 NMR spectrometer operating at 299.9 MHz (^1H), 75.4 MHz (^{13}C) and 121.4 MHz (^{31}P), a Varian UNITYINOVA 400 spectrometer operating at 399.9 MHz (^1H), 100.6 MHz (^{13}C) and 161.9 MHz (^{31}P) or on Bruker Avance (III) 600 spectrometer operating at 600.2 MHz (^1H) and 150.9 MHz (^{13}C); internal references for ^1H and ^{13}C were TMS for CDCl_3 solutions and *t*BuOH for D_2O solutions, and external reference for ^{31}P was 85% aq. H_3PO_4 . The ^1H and ^{31}P NMR spectra of the ligands at different pH were measured on the Varian S300 NMR spectrometer in water; pH was read by a freshly calibrated combined glass electrode directly in the NMR tube. The electrode was calibrated with commercial buffer solutions (pH 4, 7 and 10). Dilute aq. KOH and aq. HCl were used for pH adjustment. An insert tube with 85% aq. H_3PO_4 was used as reference. Solid-state $^{13}\text{C}\{^1\text{H}\}$ and $^{31}\text{P}\{^1\text{H}\}$ NMR spectra were acquired at 11.7 T on a Bruker Avance III

HD 500 US/WB NMR spectrometer in 4 mm ZrO₂ rotors. The ¹³C cross-polarise (CP) magic-angle spinning (MAS) NMR spectra were measured at a spinning frequency of 10 kHz and a contact time of 1 ms with a repetition delay of 5 s. The ³¹P MAS NMR spectra were measured at a spinning frequency of 11 kHz with a repetition delay of 10 s. External standards were used to calibrate ¹³C NMR (glycine, 176.03 ppm) and ³¹P NMR chemical shift scales (CaHPO₄, -0.6 ppm). The elemental analyses were carried out at the Institute of Macromolecular Chemistry of the Academy of Sciences of the Czech Republic (Prague). For potentiometric titrations, metal nitrates (recrystallised from deionised water) were used, and their stock solutions were standardised by titration with Na₂H₂edta according to the recommended procedure.^[79] The stock solution of nitric acid (≈0.03 M) was prepared from recrystallised KNO₃ on cation-exchange resin (Dowex 50). Carbonate-free KOH stock solution (≈0.2 M) was standardised against potassium hydrogenphthalate, and the HNO₃ solution against the KOH solution. The analytical-grade chemicals employed in the kinetic studies were purchased from Lachema (CuCl₂·2H₂O, ZnCl₂, NiCl₂·6H₂O, KCl, KOH, H₃PO₄, CH₃COOH, ClCH₂COOH) or Fluka (MES buffer). The freshly prepared solutions of CuCl₂, ZnCl₂ and NiCl₂ were standardised by chelatometry.^[79] Throughout the paper, pH means -log[H⁺].

Synthesis

Perhydro-3a-methyl-8a-(p-nitrobenzyl)-3a,5a,8a,10a-tetraazapyrenium diiodide (4): Compound **3** (10.00 g, 21.5 mmol) was suspended in anhydrous acetonitrile (100 mL). After a few minutes of stirring, an excess of methyl iodide (10.40 g, 73.3 mmol, 3.2 equiv) was added. The mixture was stirred at room temperature for 7 d. After this time, a new portion of methyl iodide (10.40 g, 73.3 mmol, 3.2 equiv) was added and the resulting suspension was stirred again at room temperature for a further 7 d. The yellow precipitate was collected by filtration, washed with anhydrous acetonitrile (40 mL) and dried in vacuo to give **4**·H₂O as a dark yellow solid (12.04 g, 87%). Elemental analysis found (calcd for C₂₀H₃₁I₂N₅O₂·H₂O, M_r = 645.3): C 37.43 (37.22), H 4.83 (5.15), N 10.76 (10.85), I 38.65 (39.33); ESI-MS (+ve): 372.8 ([M-2I]⁺, calcd 373.3); ¹H NMR (600.2 MHz, [D₆]DMSO): δ = 1.75–1.89 (m, 4H, CH₂CH₂CH₂), 2.863.64 (m, 12H, CH₂CH₂CH₂, NCH₂CH₂N), 3.68 (s, 3H, NCH₃), 4.29–4.37 (m, 4H, NCH₂CH₂N), 4.91 (s, 2H, NCH₂ arom.), 4.91 (d, 1H, ³J_{HH} = 13.8 Hz, NCHN), 5.06 (d, 1H, ³J_{HH} = 13.2 Hz, NCHN), 7.86 (d, 2H, ³J_{HH} = 8.4 Hz, arom.), 8.34 ppm (d, 2H, ³J_{HH} = 8.4 Hz, arom.); ¹³C{¹H} NMR (150.9 MHz, [D₆]DMSO): δ = 18.5, 18.7 (s, each 1C, CH₂CH₂CH₂); 39.2, 46.2, 46.4, 49.2 (s, each 1C, CH₂CH₂CH₂); 50.7 (s, 1C, NCH₃); 50.9, 59.6, 60.1, 63.7 (s, each 1C, NCH₂CH₂N); 63.8 (s, 1C, NCH₂ arom.); 74.9 (s, 1C, NCHN); 75.1 (s, 1C, NCHN); 123.8 (s, 2C, arom.); 132.9 (s, 2C, arom.); 135.0 (s, 1C, arom.); 148.7 ppm (s, 1C, arom.).

4-Methyl-11-(p-nitrobenzyl)-1,4,8,11-tetraazacyclotetradecane (5): Lithium hydroxide (5.00 g, 0.12 mol, 10.0 equiv) was added to a suspension of compound **4** (7.00 g, 10.8 mmol) in methanol (200 mL) and the mixture was stirred at room temperature for 2 d. The mixture was then concentrated to dryness under reduced pressure and the residue redissolved in water (200 mL). The solution was extracted with dichloromethane (4 × 300 mL). The organic phases were combined, dried with anhydrous Na₂SO₄ and volatile substances were evaporated under reduced pressure to dryness. The dark brown oil of crude product **5** was dissolved in a small amount of dichloromethane and impurities were filtered off. The clear solution was evaporated under pressure and dried in a desiccator over P₂O₅ to give **5**·0.4H₂O as a slowly crystallising red-brown oil (3.80 g, 98%). Elemental analysis found (calcd for C₁₈H₃₁N₅O₂·0.4H₂O, M_r = 356.7): C 60.88 (60.61), H 9.34 (8.99), N

19.29 (19.63); ESI-MS (+ve): 350.0 ([M+H]⁺, calcd 350.3); ¹H NMR (600.2 MHz, CDCl₃): δ = 1.19–1.24 (m, 4H, CH₂CH₂CH₂), 1.69 (s, 1H, CH₂NHCH₂), 1.85 (s, 1H, CH₂NHCH₂), 2.31 (s, 3H, NCH₃), 2.40–2.50 (m, 4H, CH₂CH₂CH₂), 2.54–2.60 (m, 4H, CH₂CH₂CH₂), 2.61–2.65 (m, 4H, NCH₂CH₂N), 2.68–2.76 (m, 4H, NCH₂CH₂N), 3.59 ppm (s, 2H, NCH₂ arom.), 7.49 ppm (d, 2H, arom., ³J_{HH} = 8.4 Hz), 8.11 (d, 2H, arom., ³J_{HH} = 8.4 Hz); ¹³C{¹H} NMR (150.9 MHz, CDCl₃): δ = 25.9, 26.0 (s, each 1C, CH₂CH₂CH₂); 29.8 (s, 1C, NCH₃); 43.1, 47.5, 47.6, 49.7 (s, each 1C, CH₂CH₂CH₂); 51.5, 53.3, 54.6, 58.0 (s, each 1C, NCH₂CH₂N); 58.4 (s, 1C, NCH₂ arom.); 123.5 (s, 2C, arom.); 129.4 (s, 2C, arom.); 147.0 (s, 1C, arom.); 147.2 ppm (s, 1C, arom.).

4-Methyl-11-(p-nitrobenzyl)-1,4,8,11-tetraazacyclotetradecane-1,8-bis(methylenephosphinic acid) (6): Amine **5** (2.00 g, 5.6 mmol) and 50% aq. hypophosphorous acid (7.50 g, 0.11 mol, 20.0 equiv) were mixed in water (20 mL). The mixture was heated to 40 °C with stirring, and solid paraformaldehyde (0.60 g, 3.0 equiv) was added in small portions over 60 min. The mixture was further heated at this temperature for 5 d. Excess paraformaldehyde was then filtered off. After concentration to a small volume under reduced pressure, the reaction mixture was purified on a strong cation-exchange resin (Dowex 50, H⁺ form, 300 mL). The excess of hypophosphorous acid was eluted with water (1000 mL) and the product **6** was collected by elution with conc. aq. HCl/H₂O (1/1 v/v). The fractions containing pure product were combined and the solvents were evaporated to dryness to afford compound **6** as a yellow oil (2.60 g). ESI-MS (+ve): 506.9 ([M+H]⁺, calcd 506.2), (-ve): 504.7 ([M-H]⁻, calcd 504.2); ¹H NMR (600.2 MHz, D₂O, pD = 1.1): δ = 1.72–1.76 (m, 4H, CH₂CH₂CH₂), 2.28 (s, 3H, N-CH₃), 2.56–2.89 (m, 16H, NCH₂CH₂N, CH₂CH₂CH₂), 3.80 (s, 2H, NCH₂ arom.), 7.00 (d, 1H, NCH₂PO₂H, ¹J_{PH} = 510.2 Hz), 7.05 (d, 1H, NCH₂PO₂H, ¹J_{PH} = 510.2 Hz), 7.61 (d, 2H, arom., ³J_{HH} = 7.8 Hz), 8.26 ppm (d, 2H, arom., ³J_{HH} = 7.8 Hz); ¹³C{¹H} NMR (150.9 MHz, D₂O, pD = 1.1): δ = 18.9, 19.4 (s, each 1C, CH₂CH₂CH₂); 43.3 (s, 1C, NCH₃); 46.0, 47.6, 48.1, 48.5 (s, each 1C, CH₂CH₂CH₂); 49.8, 51.3, 51.5, 52.6 (s, each 1C, NCH₂CH₂N); 56.5 (d, 1C, NCH₂PO₂H, ¹J_{CP} = 103 Hz); 56.9 (d, 1C, NCH₂PO₂H; ¹J_{CP} = 104 Hz); 58.7 (s, 1C, NCH₂ arom.); 123.4 (s, 2C, arom.); 130.8 (s, 2C, arom.); 145.9 (s, 1C, arom.); 147.1 (s, 1C, arom.); ³¹P{¹H} NMR (121.4 MHz, D₂O, pD = 1.1): δ = 21.2 (s); 21.7 ppm (s).

4-Methyl-11-(p-aminobenzyl)-1,4,8,11-tetraazacyclotetradecane-1,8-bis(methylenephosphinic acid) (H₂L1): Method 1: Compound **6** (0.50 g) and sodium sulfide (4.82 g, 19.7 mmol, 20.0 equiv) were dissolved in water (20 mL) and the solution was heated at 50 °C for 3 d. After concentration to a small volume under reduced pressure, the residue was purified on a silica gel column (60 mL). The column was eluted with *i*PrOH/conc. aq. NH₃/H₂O (7/3/3), and the excess of sodium sulfide and other impurities were eluted first, followed by H₂L1. Fractions containing the ligand (checked by ³¹P NMR) were combined and concentrated under reduced pressure. The residue was purified on a weak cation-exchange resin (Amberlite CG50, H⁺ form, 300 mL). Impurities were eluted with water (500 mL), and the product H₂L1 was collected by using 3% aq. HCl as eluent (500 mL). The fractions containing pure product were combined, and the solvent was evaporated to dryness in vacuo. The residue was further purified (to remove residual ammonia) on a strong cation-exchange resin (Dowex 50, H⁺ form, 300 mL) by elution with water followed by 5% aq. pyridine. Pyridine-containing fractions were combined and evaporated to dryness to afford H₂L1·2.5H₂O as a yellow oil (350 mg, 68%).

Method 2: Nickel(II) chloride hexahydrate (117 mg, 0.49 mmol, 0.1 equiv) was dissolved in water (15 mL) under argon atmosphere. After few minutes, sodium borohydride (188 mg, 4.9 mmol, 1.0 equiv) was added. A solution of compound **6** (2.50 g, 5.0 mmol)

in water/ethanol (1/1, 50 mL) alkalisied to pH \approx 8 with NaOH was added into the suspension of nickel metal. After 2 h, another portion of sodium borohydride (0.95 g, 5.0 equiv) was added, and the reaction mixture was stirred at room temperature under an argon atmosphere for 24 h. The reaction mixture was vacuum-filtered through a bed of silica gel and the product (**H₂L1**) was eluted with H₂O/EtOH (1/1 v/v). The filtrate was concentrated to a small volume in vacuo and the residue was purified on a strong cation-exchange resin (Dowex 50, H⁺ form, 300 mL). Impurities were eluted with water (500 mL) and the product was collected with 5% aq. pyridine. The pyridine-containing fractions were combined and evaporated to dryness to afford **H₂L1**·2.5H₂O as a yellow oil (1.00 g, 40%).

Elemental analysis found (calcd for C₂₀H₃₉N₅O₈P₂·2.5H₂O, M_r = 520.5): C 46.52 (46.15), H 8.82 (8.52), N 13.43 (13.45), P 12.18 (11.90); ESI-MS (–ve): 474.3 ([M–H][–], calcd 474.5); MS spectra are shown in Figure S17 (Supporting Information); ¹H NMR (600.2 MHz, D₂O, pD = 7.5): δ = 1.94–2.82 (m, 4H, CH₂CH₂CH₂), 2.86 (s, 3H, NCH₃), 2.99–3.58 (m, 16H, NCH₂CH₂N, CH₂CH₂CH₂), 4.28 (dd, 2H, NCH₂ arom.), 6.47 (d, 1H, NCH₂PO₂H, ¹J_{PH} = 511.9 Hz), 6.89 (d, 2H, arom., ³J_{HH} = 8.4 Hz), 7.31 (d, 2H, arom., ³J_{HH} = 8.4 Hz), 7.32 ppm (d, 1H, NCH₂PO₂H, ¹J_{PH} = 511.9 Hz); ¹³C{¹H} NMR (150.9 MHz, D₂O, pD = 7.5): δ = 22.8, 22.9 (s, each 1C, CH₂CH₂CH₂); 41.8, 42.4 (s, each 1C, CH₂CH₂CH₂); 47.5 (d, 1C, NCH₂PO₂H, ¹J_{CP} = 42 Hz); 47.8 (s, 1C, NCH₃); 50.5 (d, 1C, NCH₂PO₂H, ¹J_{CP} = 42 Hz); 52.3, 53.5 (s, each 1C, CH₂CH₂CH₂); 54.2, 54.6, 55.9, 56.6 (s, each 1C, NCH₂CH₂N); 57.0 (s, 1C, NCH₂ arom.); 117.1 (s, 2C, arom.); 118.5 (s, 2C, arom.); 133.9 (s, 1C, arom.); 148.9 (s, 1C, arom.); ³¹P NMR (121.4 MHz, D₂O, pD = 7.5): δ = 22.4 (dt, ¹J_{PH} = 552 Hz); 26.6 ppm (dt, ¹J_{PH} = 552 Hz); NMR spectra are shown in Figures S18–S20 (Supporting Information).

4-Methyl-11-(p-nitrobenzyl)-1,4,8,11-tetraazacyclotetradecane-1,8-bis(methylenephosphonic acid diethyl ester) (7): Compound **5** (1.95 g, 5.5 mmol) and triethyl phosphite (10.00 g, 60.2 mmol, 11.0 equiv) were mixed and the mixture was heated to 65 °C with stirring. Solid paraformaldehyde (0.80 g, 3.2 equiv) was added in small portions over 60 min. The mixture was heated at this temperature for 5 d in a closed flask. The excess paraformaldehyde was filtered off and the reaction mixture was purified on a strong cation exchange resin (Dowex 50, H⁺ form, 300 mL). The excess of triethyl phosphite was eluted with water/ethanol (1/1 v/v, 1000 mL) and the product was collected by using EtOH/conc. aq. NH₃ (5/1) as the eluent (500 mL). The fractions containing pure product were combined and the solvent was evaporated to dryness to afford **7** as a yellow oil (2.94 g). ESI MS (+): 651.0 ([M+H]⁺, calcd 651.3); ¹H NMR (600.2 MHz, [D₆]DMSO): δ = 1.13–1.25 ppm (m, 12H, POCH₂CH₃), 1.53–1.57 (m, 4H, CH₂CH₂CH₂), 2.14 (s, 3H, NCH₃), 2.32–2.68 (m, 16H, CH₂CH₂CH₂, NCH₂CH₂N) 2.75–2.84 (m, 4H, NCH₂P), 3.63 (s, 2H, NCH₂ arom.), 3.89–4.02 (m, 8H, POCH₂CH₃), 7.62 (d, 2H, arom., ³J_{HH} = 8.4 Hz), 8.17 ppm (d, 2H, arom., ³J_{HH} = 8.4 Hz); ¹³C{¹H} NMR (150.9 MHz, [D₆]DMSO): δ = 16.8 (d, 4C, POCH₂CH₃, ³J_{CP} = 6 Hz); 24.0, 24.3 (s, each 1C, CH₂CH₂CH₂); 43.1 (s, 1C, NCH₃); 49.5 (d, 1C, NCH₂P, ¹J_{CP} = 59 Hz); 50.6 (d, 1C, NCH₂P, ¹J_{CP} = 60 Hz); 51.0, 51.7, 52.1, 52.2 (s, each 1C, CH₂CH₂CH₂); 52.4, 52.5, 54.6, 55.1 (s, each 1C, NCH₂CH₂N); 57.8 (s, 1C, NCH₂ arom.); 61.6 (d, 4C, POCH₂CH₃, ²J_{CP} = 10 Hz); 123.5 (s, 2C, arom.); 130.2 (s, 2C, arom.); 146.8 (s, 1C, arom.); 149.2 ppm (s, 1C, arom.); ³¹P{¹H} NMR (121.4 MHz, [D₆]DMSO): δ = 21.4 (s), 22.6 ppm (s).

4-Methyl-11-(p-nitrobenzyl)-1,4,8,11-tetraazacyclotetradecane-1,8-bis(methylenephosphonic acid) (8): Tetraester **7** (2.92 g) was dissolved in anhydrous acetonitrile (100 mL) and the flask was wrapped in aluminium foil. Trimethylsilyl bromide (13.70 g, 90.0 mmol, 20.0 equiv) was added dropwise over 60 min and the reaction mixture was stirred in the dark at room temperature for

24 h. After concentration to a small volume under reduced pressure, the reaction mixture was dissolved in anhydrous acetonitrile (50 mL), and the resulting solution was poured into water (400 mL) with stirring. The mixture was evaporated to dryness under reduced pressure and the residue was dissolved in a small amount of water/conc. aq. HBr (1/1, three times). The residue was dissolved in conc. aq. HBr and product **8** was precipitated on addition of ethanol, collected by filtration, washed with ethanol and dried under reduced pressure in a desiccator over P₂O₅ to give **8**·3HBr·2H₂O as a pale brown solid (2.80 g, 77% based on **5**). Elemental analysis found (calcd for C₂₀H₃₇N₅O₈P₂·3HBr·2H₂O, M_r = 816.3): C 29.62 (29.43), H 5.62 (5.43), N 8.08 (8.58), P 7.59 (7.48), Br 27.39 (29.37); ESI-MS (+ve): 538.2 ([M+H]⁺, calcd 538.2), (–ve): 536.7 ([M–H][–], calcd 536.2); ¹H NMR (600.2 MHz, D₂O, pD = 1.1): δ = 1.70–1.73 (m, 4H, CH₂CH₂CH₂), 2.27 (s, 3H, NCH₃), 2.53–2.92 (m, 16H, NCH₂CH₂N, CH₂CH₂CH₂), 3.70 (d, 4H, NCH₂P, ²J_{PH} = 9.1 Hz) 3.81 (s, 2H, NCH₂ arom.), 7.61 (d, 2H, arom., ³J_{HH} = 7.8 Hz), 8.24 ppm (d, 2H, arom., ³J_{HH} = 7.8 Hz); ¹³C{¹H} NMR (150.9 MHz, D₂O, pD = 1.1): δ = 18.7, 19.8 (s, each 1C, CH₂CH₂CH₂); 43.1 (s, 1C, NCH₃); 46.3, 47.6, 47.7, 47.8 (s, each 1C, CH₂CH₂CH₂); 49.2, 50.1, 51.0, 52.6 (s, each 1C, NCH₂CH₂N); 54.3 (d, 2C, NCH₂P, ¹J_{CP} = 140 Hz); 54.7 (d, 2C, NCH₂P, ¹J_{CP} = 142 Hz); 58.4 (s, 1C, NCH₂ arom.); 123.6 (s, 2C, arom.); 130.7 (s, 2C, arom.); 145.6 (s, 1C, arom.); 146.8 ppm (s, 1C, arom.); ³¹P{¹H} NMR (121.4 MHz, D₂O, pD = 1.1): δ = 12.9 ppm (s).

4-Methyl-11-(p-aminobenzyl)-1,4,8,11-tetraazacyclotetradecane-1,8-bis(methylenephosphonic acid) (H₄L2): Nickel(II) chloride hexahydrate (66 mg, 0.28 mmol, 0.1 equiv) was dissolved in water (10 mL). After few minutes, sodium borohydride (88 mg, 0.9 mmol, 1.0 equiv) was added. A solution of compound **8** (2.00 g, 2.5 mmol) in water/ethanol (1/1, 40 mL) was alkalisied to pH \approx 8 with NaOH and added to the suspension of nickel metal. After 2 h, an excess of sodium borohydride (0.46 g, 5.0 equiv) was added and the reaction mixture was stirred at room temperature under an argon atmosphere for 24 h. The reaction mixture was vacuum-filtered through a bed of silica gel and the product was eluted with H₂O/EtOH (1/1 v/v). The eluate was concentrated to a small volume under reduced pressure, and the residue was purified on a strong cation-exchange resin (Dowex 50, H⁺ form, 300 mL). Impurities were eluted with water (500 mL) and the product was collected with 5% aq. pyridine (500 mL). The pyridine-containing fractions were evaporated to dryness to afford **H₄L2**·3H₂O as a yellow oil (900 mg, 65%). Elemental analysis found (calcd for C₂₀H₃₉N₅O₆P₂·3H₂O, M_r = 561.6): C 42.74 (42.78), H 8.08 (8.08), N 12.58 (12.47), P 11.57 (11.03); EIS-MS (–ve): 506.2 ([M–H]⁺, calcd 506.2); MS spectra are shown in Figure S21 (Supporting Information); ¹H NMR (600.2 MHz, D₂O, pD = 5.3): δ = 1.75–2.50 (m, 4H, CH₂CH₂CH₂), 2.60 (s, 3H, NCH₃), 2.67–3.30 (m, 16H, NCH₂CH₂N, CH₂CH₂CH₂), 3.44 (s, 2H, NCH₂ arom.), 4.10 (s, 2H, NCH₂PO₃H₂), 4.17 (s, 2H, NCH₂PO₃H₂), 6.80 (d, 2H, arom., ³J_{HH} = 7.8 Hz), 7.21 ppm (d, 2H, arom., ³J_{HH} = 8.4 Hz); ¹³C{¹H} NMR (150.9 MHz, D₂O, pD = 5.3): δ = 22.2, 22.3 (s, each 1C, CH₂CH₂CH₂); 41.1 (s, 1C, NCH₃); 47.0, 47.1, 47.3, 49.5 (s, each 1C, CH₂CH₂CH₂); 49.8 (d, 1C, NCH₂PO₃H₂, ¹J_{CP} = 88 Hz); 50.8 (d, 1C, NCH₂PO₃H₂, ¹J_{CP} = 97 Hz); 50.3, 54.0, 54.8, 55.3 (s, each 1C, NCH₂CH₂N); 56.2 (s, 1C, NCH₂ arom.); 116.8 (s, 2C, arom.); 118.7 (s, 2C, arom.); 133.1 (s, 1C, arom.); 146.8 ppm (s, 1C, arom.); ³¹P NMR (121.4 MHz, D₂O, pD = 5.3): δ = 20.9 (s), 21.2 ppm (s); NMR spectra are shown in Figures S22–S24 (Supporting Information).

X-ray diffraction

Single crystals of bis-quaternary salt **4**·EtOH were prepared by diffusion of ethanol vapour into an aqueous solution of **4** (saturated in hot water). Single crystals of 1,8-bis(p-nitrobenzyl)cyclam and

compound **5** were obtained by slow evaporation of ethanolic solutions of the corresponding compounds. Selected crystals were mounted on a glass fibre in random orientation and the diffraction data were acquired at 150(1) K (Cryostream Cooler, Oxford Cryosystems) with $\text{MoK}\alpha$ radiation ($\lambda = 0.71073 \text{ \AA}$). In the cases of 1,8-bis(*p*-nitrobenzyl)cyclam and **4**•EtOH, data were collected on a Nonius Kappa CCD diffractometer (Enraf-Nonius) and analysed with the HKL DENZO program package.^[80] The structures were solved by direct methods and refined by full-matrix least-squares techniques by using SIR92^[81] and SHELXL97^[82] programs. The diffraction data of compound **5** were collected on an ApexII CCD diffractometer and analysed by using the SAINT V8.27B (Bruker AXS Inc., 2012) program package. The structure was solved by direct methods (SHELXS97^[83]) and refined by full-matrix least-squares techniques (SHELXL97^[82]). For compound **4**•EtOH, absorption correction by Gaussian integration^[84] was applied. In general, all non-hydrogen atoms in positions with full occupancy were refined anisotropically. Although hydrogen atoms could usually be found in the electron difference map, they were fixed in original (those bound to nitrogen atoms) or theoretical (those belonging to carbon atoms) positions by using a riding model with $U_{\text{eq}}(\text{H}) = 1.2 U_{\text{eq}}(\text{X})$ to keep the number of refined parameters low.

In the case of 1,8-bis(*p*-nitrobenzyl)cyclam, two centrosymmetric molecules are present in the unit cell, that is, two half-molecules form the independent unit. For one of them, a disorder of the macrocyclic part was found. It was best modelled with two possible arrangements of the macrocycle with relative occupancy 90:10 (Supporting Information, Figure S1). Disordered parts of the macrocycle in both positions share the same (undisordered) nitrobenzyl side group. Atoms belonging to part of the macrocycle with higher occupancy were refined in anisotropic mode, and those with lower occupancy were refined isotropically. For compound **4**•EtOH, the independent unit consists of one formula unit, that is, one bis-quaternary cation, two iodide anions and an ethanol molecule of solvation. The benzyl group was found to be twisted in two positions sharing the same pivot methylene group. Both possibilities have approximately the same occupancy (refined ratio 52:48), and the corresponding disordered atoms were refined isotropically (Supporting Information Figure S2). The ethanol molecule of solvation was located in the electron density map, but it was heavily disordered and the irregularity could not be sufficiently modelled (the presence of ethanol was confirmed by ¹H NMR spectroscopy). Therefore, the ethanol molecule was squeezed by using PLATON.^[85] The number of squeezed electrons corresponded well with the electron count of one ethanol molecule. For compound **5**, one molecule forms the independent unit. A part of the macrocycle was disordered and best fitted with relative occupancy 80:20 (Supporting Information, Figure S3). Atoms in positions with higher occupancy were refined anisotropically, and those with lower occupancy were refined isotropically.

Selected experimental data are listed in Table 10. CCDC 1019313 (1,8-bis(*p*-nitrobenzyl)cyclam), 1019312 (**4**•EtOH) and 1019311 (**5**) contain the supplementary crystallographic data for this paper. These data can be obtained free of charge from The Cambridge Crystallographic Data Centre via www.ccdc.cam.ac.uk/data_request/cif.

Potentiometry

In general, the experiments followed a procedure published elsewhere.^[32] The equilibria in $\text{M}^{\text{II}}\text{-H}_2\text{L1/H}_4\text{L2}$ systems were established slowly, and therefore an out-of-cell technique was used with waiting times of 5 d ($\text{Cu}^{\text{II}}\text{-H}_2\text{L1/H}_4\text{L2}$ and $\text{Zn}^{\text{II}}\text{-H}_2\text{L1}$ systems) and six

Table 10. Selected crystallographic data.

Parameter	1,8-bis(<i>p</i> -nitrobenzyl)-cyclam	4 •EtOH	5
formula	$\text{C}_{24}\text{H}_{34}\text{N}_6\text{O}_4$	$\text{C}_{22}\text{H}_{37}\text{I}_2\text{N}_5\text{O}_3$	$\text{C}_{18}\text{H}_{31}\text{N}_5\text{O}_2$
M_r	470.57	673.37	349.48
colour, habit	yellow prism	yellow prism	yellow, irregular
crystal system	triclinic	monoclinic	orthorhombic
space group	$P\bar{1}$	$P2_1/c$	$P2_12_12_1$
a [Å]	7.4190(3)	12.2995(4)	9.0984(7)
b [Å]	7.7962(3)	19.2331(6)	9.7822(6)
c [Å]	21.2206(6)	10.9595(3)	21.9209(15)
α [°]	93.533(2)	90	90
β [°]	90.674(2)	96.9690(10)	90
γ [°]	99.092(2)	90	90
V [Å ³]	1209.39(8)	2573.40(14)	1951.0(2)
Z	2	4	4
ρ_{calcd} [g cm ⁻³]	1.292	1.738	1.190
μ [mm ⁻¹]	0.090	2.476	0.080
unique reflns	5482	5910	3819
obsd reflns	3957	5304	3230
$[I > 2\sigma(I)]$			
$R; R' [I > 2\sigma(I)]$	0.0649; 0.0425	0.0320; 0.0273	0.0788; 0.0655
$wR; wR' [I > 2\sigma(I)]$	0.1208; 0.1109	0.0585; 0.0569	0.1366; 0.1314

weeks ($\text{Ni}^{\text{II}}\text{-H}_2\text{L1/H}_4\text{L2}$ systems) to establish full equilibrium. Then, the potential at each titration point (tube) was determined with a freshly calibrated electrode. For the $\text{Zn}^{\text{II}}\text{-H}_4\text{L2}$ system, the equilibrium was established relatively quickly at each titration point (≤ 4 min), and thus $\text{Zn}^{\text{II}}\text{-H}_4\text{L2}$ was studied by conventional titrations. The titrations were carried out in a thermostatted vessel at $25.0 \pm 0.1^\circ\text{C}$ at a constant ionic strength of $I(\text{KNO}_3) = 0.1 \text{ M}$. The concentration of ligands in the titration vessel was about 0.004 M . The metal:ligand ratio was 1:1 in all cases. The initial volume was about 1 cm^3 for out-of-cell titrations and about 5 cm^3 for the conventional ones. The measurements were taken with an excess of HNO_3 added to the initial mixture. The mixtures were titrated with stock KOH solution in the pH range 1.7–7.1 for out-of-cell (25 points per each titration) and 1.8–11.9 for conventional (40 data points per titration) titrations. Titrations for each system were carried out four times. An inert atmosphere was ensured by a constant flow of argon saturated with water vapour. The constants with their standard deviations were calculated by using the OPIUM program package^[86] and are concentration constants defined as $\beta_h = [\text{H}_h\text{L}]/([\text{H}]^h[\text{L}])$; they can be transformed into the protonation constants $\log K_h$ ($\log K_1 = \log \beta_1$, and in general $\log K_h(\text{H}_h\text{L}) = \log \beta_h - \log \beta_{(h-1)}$). Note that $\log K_h = \text{p}K_{\text{A}}$ of corresponding protonated species. The concentration stability constants β_{hlm} are defined as $\beta_{\text{hlm}} = [\text{H}_h\text{L}_m\text{M}_m]/([\text{H}]^h[\text{L}]^m[\text{M}]^m)$. The ionic product of water used in the calculations was $\text{p}K_{\text{w}} = 13.78$.

Kinetic measurements

In general, experiments were run according to the published procedures.^[26,35] The experiments on the kinetics of formation were carried out under pseudo-first-order conditions with fiftyfold excess of CuCl_2 ($c_{\text{Cu}} = 5 \text{ mM}$, $c_{\text{L}} = 116 \mu\text{M}$ for $\text{H}_2\text{L1}$, $c_{\text{L}} = 100 \mu\text{M}$ for $\text{H}_4\text{L2}$). The acidity/basicity was controlled by chloroacetate, acetate, phosphate (conventional UV/Vis experiments) or MES (stopped-flow experiments) buffers (0.01 M). Influence of the buffer anions

on the complexation reaction was checked by measurement of k_{obs} at various buffer concentrations (range 0.006–0.03 M) at a constant pH of 3.18 (Supporting Information, Figure S8). All experiments were carried out at $25.0 \pm 0.1^\circ\text{C}$ and $I = 0.1\text{ M}$ (KCl). A conventional diode-array spectrophotometer (Shimadzu UV-2401PC) was used for measurements in the pH range in which the reaction was slow (pH 2.4–5.0 for $\text{Cu}^{\text{II}}\text{-H}_2\text{L1}$ and pH 2.4–4.1 for $\text{Cu}^{\text{II}}\text{-H}_4\text{L2}$). A stopped-flow spectrometer (Applied Photophysics SX.18MV) was used at the higher pH (pH 5.2–7.3 for $\text{Cu}^{\text{II}}\text{-H}_2\text{L1}$ and pH 4.5–7.0 for $\text{Cu}^{\text{II}}\text{-H}_4\text{L2}$). The complexation reaction was monitored directly by means of the increase of the CT band ($\lambda = 310\text{ nm}$) of the $\text{Cu}\text{-L}$ complexes. The k_{obs} value was obtained by fitting the data with the equation $A(t) = A_{\infty}[1 - \exp(-k_{\text{obs}}t)]$. An example of the data fitting is shown in Figure S25 of the Supporting Information.

The dissociation kinetics were studied in the $[\text{H}^+]$ range of 0.025–4.89 M at $I = 5.0\text{ M}$ (H_2NaClO_4), with a starting concentrations of $\text{Cu}^{\text{II}}\text{-H}_2\text{L1}$ and $\text{Cu}^{\text{II}}\text{-H}_4\text{L2}$ complexes of 7.4 and 5.9 mM, respectively in the temperature range $25\text{--}55^\circ\text{C}$. The reactions were monitored by means of the decrease in intensity of the CT band ($\lambda = 310\text{ nm}$) of the complexes with time. The kinetic measurements were carried out with a conventional diode-array spectrophotometer (Shimadzu UV-2401PC, temperature-controlled by Peltier thermoelectric heating to $(25\text{--}55) \pm 0.1^\circ\text{C}$). The k_{obs} values were calculated from the experimental data by using a single-exponential model $A(t) = A_0 \exp(-k_{\text{obs}}t)$. An example of data fitting is shown in Figure S26 (Supporting Information). Fitting of pH and temperature dependences of the formation and dissociation rate constants was performed by using a MicroMath Scientist program^[87] with the $1/y^2$ weighting scheme.

Formation experiments with simple ligands were also performed in the presence of ^{64}Cu . The ligands were radiolabelled by adding 1–2 MBq of ^{64}Cu to $10\ \mu\text{g}$ of $\text{H}_2\text{L1}$, $\text{H}_4\text{L2}$, cyclam and *N*-benzylcyclam dissolved in $100\ \mu\text{L}$ of 0.05 M MES/NaOH buffer (pH 5.5). The radiolabelling yield as function of time was determined by radio-TLC. Radio-TL chromatograms were scanned with a radioisotope thin-layer analyzer (Rita Star, Raytest). For $\text{H}_2\text{L1}$, $\text{H}_4\text{L2}$: silica gel plates (Merck, F254) as stationary phase, 1 M aq. triethylammonium hydrogencarbonate/methanol (3/1, v/v) as eluent; $^{64}\text{CuCl}_2$, $R_f = 0$; $^{64}\text{Cu-L1}$, $R_f = 0.6$; $^{64}\text{Cu-L2}$, $R_f = 0.65$. Cyclam, *N*-benzylcyclam: iTLC-SA strips (Agilent) as stationary phase, 0.1 M aq. ethylenediaminetetraacetic acid (EDTA) as mobile phase; free ^{64}Cu as $^{64}\text{Cu-EDTA}$, $R_f = 0.9\text{--}1.0$; $^{64}\text{Cu-cyclam}$ and $^{64}\text{Cu-N-benzylcyclam}$, $R_f = 0$.

Synthesis of polymer-supported macrocyclic ligands

Poly(glycidyl methacrylate-co-ethylene dimethacrylate) macroporous beads (60:40 w/w, 20–40 μm , 8.0 g, 32 mmol epoxide groups)^[75] in solution of 1,3-benzenediol (resorcinol, 16.0 g, 145 mmol) and sodium hydroxide (2.9 g, 73 mmol) in *N,N*-dimethylacetamide (30 mL) were heated at 100°C with stirring by anchor stirrer for 5 h. The resorcinol-modified polymer (GMA-resorcinol) was washed subsequently with methanol (250 mL), 5% aq. acetic acid (200 mL) and methanol (300 mL) and dried in air (yield 8.2 g). Elemental analysis found: C 56.35, H 7.96, N 1.32; $^{13}\text{C}\{^1\text{H}\}$ CP-MAS NMR (125.8 MHz): $\delta = 19.8$ (aliph.), 45.5 (aliph.), 56.5 (aliph.), 63.0 (aliph.), 104.5 (arom.), 130.5 (arom.), 159.9 (arom.), 179.0 ppm (C=O). The content of resorcinol was calculated on the basis of ^{13}C solid-state NMR data and was found to be 0.974 mmol g^{-1} .

The polymer with immobilised resorcinol (200 mg) was added to solution of sodium carbonate (2.7 g, 25 mmol) in water (60 mL). Ligand $\text{H}_2\text{L1}$ or $\text{H}_4\text{L2}$ (80 mg, $\approx 0.15\text{ mmol}$) was dissolved in aq. HCl (6 M, 2.0 mL). Sodium nitrite (11.4 mg, 0.17 mmol) was dissolved in water (0.9 mL). Urea (27 mg, 0.45 mmol) was dissolved in water

(0.9 mL). All following reactions were carried out at -5 to 0°C . The solution of sodium nitrite was added to the solution of a ligand. After diazotisation for 10 min, the solution of urea was added, the solution was left to stand for 5 min and then added to the stirred suspension of the resorcinol-modified polymer in aq. sodium carbonate. After 2 h, the modified polymer was centrifuged off, washed with water (150 mL) and methanol (50 mL) and dried in air. Typical yield was 200 mg.

resin- $\text{H}_2\text{L1}$ (GMA-phosphinate): Elemental analysis: P 0.40% ($129\ \mu\text{mol g}^{-1}$, corresponds to $65\ \mu\text{mol}$ of the ligand per 1 g of resin); $^{13}\text{C}\{^1\text{H}\}$ CP-MAS NMR (125.8 MHz): $\delta = 20.0$ (aliph.), 46.8 (aliph.), 53.2 (aliph.), 66.0 (aliph.), 104.5 (arom.), 130.5 (arom.), 160.0 (arom.), 178.0 (C=O); $^{31}\text{P}\{^1\text{H}\}$ CP-MAS NMR (202.4 MHz): $\delta = 21\text{ ppm}$ (br).

resin- $\text{H}_4\text{L2}$ (GMA-phosphonate): Elemental analysis: P: 0.27% ($87\ \mu\text{mol g}^{-1}$, corresponds to $44\ \mu\text{mol}$ of the ligand per 1 g of the resin); $^{13}\text{C}\{^1\text{H}\}$ CP-MAS NMR (125.8 MHz): $\delta = 18.5$ (aliph.), 46.0 (aliph.), 54.5 (aliph.), 65.5 (aliph.), 103.0 (arom.), 129.7 (arom.), 160.0 (arom.), 177.5 ppm (C=O); $^{31}\text{P}\{^1\text{H}\}$ CP-MAS NMR (202.4 MHz): $\delta = 18\text{ ppm}$ (br).

Separation of copper(II) from Ni^{II}/Zn^{II}

The chelating polymer resin (resin- $\text{H}_2\text{L1}$ or resin- $\text{H}_4\text{L2}$, 20 mg) was added to a mixture of stock solutions of the metal ions (0.700 mL; see below for composition) and buffer (0.700 mL, pH 3.0 or 5.0; see below for composition). The suspension was shaken for 1 h at room temperature and centrifuged. The supernatant was analysed for metal content by AAS. The pellet was redispersed in washing buffer (pH 3.0, 1.4 mL, 1st wash; see below for composition), incubated for 20 min at room temperature and centrifuged, and the supernatant was taken for AAS. Washing with the buffer (pH 3.0, 1.4 mL) was repeated once more (2nd wash, the supernatant was taken for AAS analysis of metal contents). Desorption of the chelated copper was performed by incubation of the loaded polymer with aq. HCl (1 M, 1.4 mL) for 20 min at room temperature followed by centrifugation (the supernatant was taken for AAS analysis of metal contents, 1st desorption). The desorption step was repeated once more (2nd desorption).

The Ni + Cu stock solution was prepared by dissolution of nickel(II) chloride hexahydrate (810 mg, 3.4 mmol) and copper(II) sulfate pentahydrate (1.6 mg, 0.0064 mmol) in water, and the total volume was adjusted with water to 10.0 mL ($c_{\text{Cu}} = 0.04\text{ mg mL}^{-1}$, $c_{\text{Ni}} = 20\text{ mg mL}^{-1}$). The Zn + Cu stock solution was prepared by dissolution of zinc(II) chloride (464 mg, 3.4 mmol) and copper(II) sulfate pentahydrate (1.6 mg, 0.0064 mmol) in water, and the total volume was adjusted with water to 10.0 mL ($c_{\text{Cu}} = 0.04\text{ mg mL}^{-1}$, $c_{\text{Zn}} = 22\text{ mg mL}^{-1}$). The chloroacetate buffer stock solution (pH 3.0) was prepared by dissolution of chloroacetic acid (8.03 g, 85 mmol) in water (ca 25 mL), titration with aq. NaOH (50 wt.%) to pH 3.0 and adjustment of total volume to 50.0 mL ($c_{\text{buffer}} = 1.7\text{ M}$). The acetate buffer stock solution (pH 5.0) was prepared by dissolution of acetic acid (5.10 g, 85 mmol) in water (ca 25 mL), titration with aq. NaOH (50 wt.%) to pH 5.0 and adjustment of total volume to 50.0 mL ($c_{\text{buffer}} = 1.7\text{ M}$). The wash buffer (pH 3.0) was prepared by dilution of the chloroacetate buffer stock solution having pH 3.0 with water (1/1 v/v).

Separation of radiocopper(II) from nickel

Intensity of radioactive decay was determined by using an Isomed 2000 activimeter (MED, Nuclear-Medizintechnik GmbH, Dresden, Germany). ICP-MS was performed on a Sektorfeld-ICP-Mass spec-

trometer Element2 (ThermoFisher Scientific) after complete decay of radioactivity. Aq. HCl (30%, Suprapur) was purchased from Merck-Millipore, and MES from Applichem. Each step was performed under metal-free conditions. Double-distilled water was used for dilution of HCl (30%) as well as for preparation of the MES buffer solution.

Starting ^{64}Cu solution in 0.01 M aq. HCl was prepared as described previously.^[78] To 2.59 mL of this solution, a defined amount of nickel was added (10 μL of the stock solution of NiSO_4 containing 2.6 mg mL^{-1} of Ni), resulting in a final radiocopper solution with Ni concentration of 10 000 $\mu\text{g L}^{-1}$, which was used in the sorption experiments.

The resins were pretreated by the following procedure: 1 mg of resin was incubated in aq. HCl (1 M) for 24 h. After separation of the resin by centrifugation, the content of Ni/Cu/Zn in the supernatant was determined by ICP-MC to determine threshold/background level. Subsequently, the resin was washed three times with MES buffer (0.1 M, pH 5.5).

Adsorption of ^{64}Cu was studied by following procedure: 20 μL of ^{64}Cu solution (the starting activity was 51.5 and 52.2 MBq for resin-H₂L1 and resin-H₄L2, respectively) was added to MES buffer (980 μL , 0.1 M, pH 5.5). These solutions were added to 1 mg of resin (pretreated with HCl). After shaking at room temperature for 30 min and subsequent centrifugation, the supernatant was removed and its radioactivity was determined. In addition, the resin was further washed three times with MES buffer (1 mL, 0.1 M, pH 5.5).

Desorption of ^{64}Cu was performed in the following way: 1 M aq. HCl (1 mL) was added to the loaded resin. After shaking at room temperature for 15 min and subsequent centrifugation, the supernatant was removed and the resin was washed three times with 1 M aq. HCl (1 mL). Supernatants were further analysed to determine radioactivity level and by ICP-MS.

Acknowledgements

We thank Dr. K. Lang (Institute of Inorganic Chemistry, Academy of Science of the Czech Republic) for the use of a stopped-flow apparatus, Ing. O. Policianova (Institute of Macromolecular Chemistry, Academy of Science of the Czech Republic) for measuring of solid-state NMR spectra, and Dr. M. Kubeil, C. Jentschel and R. A. Nadar (Helmholtz-Zentrum Dresden-Rossendorf) for carrying out the radiochemical investigations. This work was supported by the Grant Agency of the Czech Republic (grants P207/11/1437 and P304/12/0950).

Keywords: copper · ion-selective resins · kinetics · macrocyclic ligands · radiochemistry

- [1] M. Meyer, V. Dahaoui-Ginderey, C. Lecomte, R. Guillard, *Coord. Chem. Rev.* **1998**, 178–180, 1313–1405.
- [2] L. F. Lindoy, *Adv. Inorg. Chem.* **1998**, 45, 75–125.
- [3] R. Delgado, V. Félix, L. M. P. Lima, D. W. Price, *Dalton Trans.* **2007**, 2734–2745.
- [4] *The Chemistry of Contrast Agents in Medical Magnetic Resonance Imaging*, 2nd ed. (Eds.: A. Merbach, L. Helm, É. Tóth), Wiley, Hoboken, **2013**.
- [5] *Topics in Current Chemistry*, Vol. 221 (Ed.: W. Krause), Springer, Heidelberg, **2002**.
- [6] S. Aime, M. Botta, E. Terreno, *Adv. Inorg. Chem.* **2005**, 57, 173–237.
- [7] P. Caravan, *Chem. Soc. Rev.* **2006**, 35, 512–523.

- [8] P. Hermann, J. Kotek, V. Kubiček, I. Lukeš, *Dalton Trans.* **2008**, 3027–3047.
- [9] C. J. Anderson, M. J. Welch, *Chem. Rev.* **1999**, 99, 2219–2234.
- [10] W. A. Volkert, T. J. Hoffmann, *Chem. Rev.* **1999**, 99, 2269–2292.
- [11] S. Liu, *Chem. Soc. Rev.* **2004**, 33, 445–461.
- [12] S. Liu, D. S. Edwards, *Bioconjugate Chem.* **2001**, 12, 7–34.
- [13] M. J. Welch, *Handbook of Radiopharmaceuticals: Radiochemistry and Applications* (Eds.: C. S. Redvanly), Wiley, Hoboken, **2003**.
- [14] W. P. Li, L. A. Meyer, C. J. Anderson, *Top. Curr. Chem.* **2005**, 252, 179–192.
- [15] T. J. Wadas, E. H. Wong, G. R. Weisman, C. J. Anderson, *Chem. Rev.* **2010**, 110, 2858–2902.
- [16] B. M. Zeglis, J. S. Lewis, *Dalton Trans.* **2011**, 40, 6168–6195.
- [17] C. S. Cutler, H. M. Hemmkens, N. Sisay, S. Huclier-Markai, S. S. Jurisson, *Chem. Rev.* **2013**, 113, 858–883.
- [18] E. W. Price, C. Orvig, *Chem. Soc. Rev.* **2014**, 43, 260–290.
- [19] S. V. Smith, *J. Inorg. Biochem.* **2004**, 98, 1874–1901.
- [20] X. Sun, C. J. Anderson, *Methods Enzymol.* **2004**, 386, 237–261.
- [21] T. J. Wadas, E. H. Wong, G. R. Weisman, C. J. Anderson, *Curr. Pharm. Des.* **2007**, 13, 3–16.
- [22] S. Thieme, M. Walther, S. Preusche, J. Rajander, H.-J. Pietzsch, O. Solin, J. Steinbach, *Appl. Radiat. Isot.* **2013**, 72, 169–176.
- [23] a) M. Sadeghi, M. Amiri, P. Rowshanfarzad, M. Avila, C. Tenreiro, *Radiochim. Acta* **2008**, 96, 399–402; b) R. Schwarzbach, K. Zimmermann, P. Blauenstein, A. Smith, P. A. Schubiger, *Appl. Radiat. Isot.* **1995**, 46, 329–336; c) S. V. Smith, D. J. Waters, N. DiBartolo, *Radiochim. Acta* **1996**, 75, 65–68.
- [24] C. Dirks, B. Scholten, S. Happel, A. Zulauf, A. Bombard, H. Jungclas, *J. Radioanal. Nucl. Chem.* **2010**, 286, 671–674.
- [25] J. Kotek, P. Vojtíšek, I. Císařová, P. Hermann, P. Jurečka, J. Rohovec, I. Lukeš, *Collect. Czech. Chem. Commun.* **2000**, 65, 1289–1316.
- [26] J. Kotek, P. Lubal, P. Hermann, I. Císařová, I. Lukeš, T. Godula, I. Svobodová, P. Táborský, J. Havel, *Chem. Eur. J.* **2003**, 9, 233–248.
- [27] I. Svobodová, P. Lubal, P. Hermann, J. Kotek, J. Havel, *J. Inclusion Phenom. Macrocyclic Chem.* **2004**, 49, 11–15.
- [28] I. Svobodová, P. Lubal, P. Hermann, J. Kotek, J. Havel, *Microchim. Acta* **2004**, 148, 21–26.
- [29] P. Lubal, J. Maleček, P. Hermann, J. Kotek, J. Havel, *Polyhedron* **2006**, 25, 1884–1892.
- [30] S. Fůzerová, J. Kotek, I. Císařová, P. Hermann, K. Binnemans, I. Lukeš, *Dalton Trans.* **2005**, 2908–2915.
- [31] T. Vitha, J. Kotek, J. Rudovský, V. Kubiček, I. Císařová, P. Hermann, I. Lukeš, *Collect. Czech. Chem. Commun.* **2006**, 71, 337–367.
- [32] I. Svobodová, P. Lubal, J. Plutnar, J. Havlíčková, J. Kotek, P. Hermann, I. Lukeš, *Dalton Trans.* **2006**, 5184–5197.
- [33] J. Plutnar, J. Havlíčková, J. Kotek, P. Hermann, I. Lukeš, *New J. Chem.* **2008**, 32, 496–504.
- [34] J. Havlíčková, H. Medová, T. Vitha, J. Kotek, I. Císařová, P. Hermann, *Dalton Trans.* **2008**, 5378–5386.
- [35] I. Svobodová, J. Havlíčková, J. Plutnar, P. Lubal, J. Kotek, P. Hermann, *Eur. J. Inorg. Chem.* **2009**, 3577–3592.
- [36] L. M. P. Lima, R. Delgado, J. Plutnar, P. Hermann, J. Kotek, *Eur. J. Inorg. Chem.* **2011**, 527–538.
- [37] G. Royal, V. Dahaoui-Gindrey, S. Dahaoui, A. Tabard, R. Guillard, P. Pulumbi, C. Lecomte, *Eur. J. Org. Chem.* **1998**, 1971–1975.
- [38] C. Bucher, G. Royal, J. M. Barbe, R. Guillard, *Tetrahedron Lett.* **1999**, 40, 2315–2318.
- [39] J. Kotek, P. Hermann, P. Vojtíšek, J. Rohovec, I. Lukeš, *Collect. Czech. Chem. Commun.* **2000**, 65, 243–266.
- [40] E. H. Wong, G. R. Weisman, D. C. Hill, D. P. Reed, M. E. Rogers, J. S. Condon, M. A. Fagan, J. C. Calabrese, K. C. Lam, I. A. Guzei, A. L. Rheingold, *J. Am. Chem. Soc.* **2000**, 122, 10561–10572.
- [41] C. Bucher, E. Duval, J.-M. Barbe, J.-N. Verpeaux, C. Amatore, R. Guillard, *C. R. Acad. Sci. Paris, Ser. II: Chim.* **2000**, 3, 211–222.
- [42] H. Kurosaki, C. Bucher, E. Espinosa, J.-M. Barbe, R. Guillard, *Inorg. Chim. Acta* **2001**, 322, 145–149.
- [43] R. Kolinski, *Pol. J. Chem.* **1995**, 69, 1039–1945.
- [44] B. Bosnich, C. K. Poon, M. Tobe, *Inorg. Chem.* **1965**, 4, 1102–1108.
- [45] G. Anderegg, F. Arnaud-Neu, R. Delgado, J. Felcman, K. Popov, *Pure Appl. Chem.* **2005**, 77, 1445–1495.

- [46] I. Lukeš, J. Kotek, P. Vojtišek, P. Hermann, *Coord. Chem. Rev.* **2001**, 216–217, 287–312.
- [47] NIST Standard Reference Database 46 (Critically Selected Stability Constants of Metal Complexes), Version 7.0, **2003**.
- [48] J. Blahut, I. Čisářová, P. Hermann, J. Kotek, unpublished results.
- [49] N. E. Good, G. D. Winget, W. Winter, T. N. Connolly, S. Izawa, R. M. M. Singh, *Biochemistry* **1966**, 5, 467–477.
- [50] A. Röhrich, R. Bergmann, A. Kretzschmann, S. Noll, H.-J. Pietzsch, J. Steinbach, H. Stephan, *J. Inorg. Biochem.* **2011**, 105, 821–832.
- [51] R. Buxtorf, T. A. Kaden, *Helv. Chim. Acta* **1974**, 57, 1035–1042.
- [52] M. Maeder, Y.-M. Neuhold, G. Puxty, P. King, *Phys. Chem. Chem. Phys.* **2003**, 5, 2836–2841.
- [53] A. P. Leugger, L. Hertli, T. A. Kaden, *Helv. Chim. Acta* **1978**, 61, 2296–2306.
- [54] M. Kodama, E. Kimura, *J. Chem. Soc. Dalton Trans.* **1977**, 1473–1478.
- [55] a) D. J. Stigers, R. Ferdani, G. R. Weisman, E. H. Wong, C. J. Anderson, J. A. Golen, C. Moore, A. L. Rheingold, *Dalton Trans.* **2010**, 39, 1699–1701; b) R. Ferdani, D. J. Stigers, A. L. Fiamengo, L. Wei, B. T. Y. Li, J. A. Golen, A. L. Rheingold, G. R. Weisman, E. H. Wong, C. J. Anderson, *Dalton Trans.* **2012**, 41, 1938–1950; c) Y. Guo, R. Ferdani, C. J. Anderson, *Bioconjugate Chem.* **2012**, 23, 1470–1477; d) M. Jiang, R. Ferdani, M. Shokeen, C. J. Anderson, *Nucl. Med. Biol.* **2013**, 40, 245–251; e) D. Zeng, Q. Ouyang, Z. Cai, X.-Q. Xie, C. J. Anderson, *Chem. Commun.* **2014**, 50, 43–45.
- [56] L.-H. Chen, C.-S. Chung, *Inorg. Chem.* **1988**, 27, 1880–1883.
- [57] Z. Y. A. Yu, R. A. Wu, M. H. Wu, L. Zhao, R. B. Li, H. F. Zou, *Colloids Surf. B* **2010**, 78, 222–228.
- [58] M. Škodová, J. Kučka, M. Vetrík, J. Skopal, Z. Walterová, O. Sedláček, P. Štěpáněk, J. Mattová, P. Poučková, P. Urbánek, M. Hrubý, *React. Funct. Polym.* **2003**, 73, 1426–1431.
- [59] K. F. Murray, D. Lam, K. V. Kowdley, *Exp. Opin. Pharmacother.* **2003**, 4, 2239–2251.
- [60] G. Crisponi, V. M. Nurchi, D. Funni, C. Gerosa, S. Nemolato, G. Faa, *Coord. Chem. Rev.* **2010**, 254, 876–889.
- [61] L. Cai, X. K. Li, Y. Song, M. G. Cherian, *Curr. Med. Chem.* **2005**, 12, 2753–2763.
- [62] P. Burke, O. Golovko, J. C. Clark, F. I. Aigbirhio, *Inorg. Chim. Acta* **2010**, 363, 1316–1319.
- [63] D. W. McCarthy, R. E. Shefer, R. E. Klinkowtein, L. A. Bass, W. H. Margeneau, C. S. Cutler, C. J. Anderson, M. J. Welch, *Nucl. Med. Biol.* **1997**, 24, 35–43.
- [64] C. M. Jeffery, S. V. Smith, A. H. Asad, S. Chan, R. I. Price, *Routine Production of Copper-64 Using 11.7 MeV Protons, Vol. 1509* (Eds.: M. A. AvilaRodriguez, J. P. O'Neil, T. E. Barnhart, D. W. Dick, J. M. Kozirowski, S. E. Lapi, J. S. Lewis), Amer Inst Physics, Melville, USA, **2012**, pp. 84–90.
- [65] C. Alliot, N. Michel, A. C. Bonraisin, V. Bosse, J. Laize, C. Bourdeau, B. M. Mokili, F. Haddad, *Radiochim. Acta* **2011**, 99, 627–630.
- [66] M. R. Awual, M. Ismael, T. Yaita, S. A. El-Safty, H. Shiwaku, Y. Okamoto, S. Suzuki, *Chem. Eng. J.* **2013**, 222, 67–76.
- [67] B. Shah, T. Chakrabarky, V. K. Shahi, U. Chudasama, *Sep. Sci. Technol.* **2013**, 48, 2382–2390.
- [68] P. K. Tapaswi, M. S. Moorthy, S. S. Park, C.-S. Ha, *J. Solid State Chem.* **2014**, 211, 191–199.
- [69] Z. Q. Wang, M. Wang, G. H. Wu, D. Y. Wu, A. G. Wu, *Dalton Trans.* **2014**, 43, 8461–8468.
- [70] M. R. Awual, I. M. M. Rahman, T. Yaita, M. A. Khaleque, M. Ferdows, *Chem. Eng. J.* **2014**, 236, 100–109.
- [71] Y. H. Zhai, D. Yang, X. J. Chang, Y. W. Liu, Q. He, *J. Sep. Sci.* **2008**, 31, 1195–1200.
- [72] M. Mureseanu, N. Cioatera, I. Trandafir, I. Georgescu, F. Fajula, A. Galarneau, *Microporous Mesoporous Mater.* **2011**, 146, 141–150.
- [73] S. Malkondu, A. Kocak, M. Yilmaz, *J. Macromol. Sci. Pure Appl. Chem.* **2009**, 46, 745–750.
- [74] S. Goubert-Renaudin, M. Etienne, Y. Rousselin, F. Denat, B. Lebeau, A. Walcarius, *Electroanalysis* **2009**, 21, 3–5.
- [75] F. Švec, J. Hradil, J. Čoupek, J. Kálal, *Angew. Makromol. Chem.* **1975**, 48, 135–143.
- [76] D. Horák, J. Straka, J. Štokr, B. Schneider, T. B. Tennikova, F. Švec, *Polymer* **1991**, 32, 1135–1139.
- [77] M. Hrubý, J. Kučka, M. Nováková, H. Macková, M. Vetrík, *Appl. Radiat. Isot. Appl. Radiat. Isotop.* **2010**, 68, 334–339.
- [78] S. Thieme, M. Walther, H.-J. Pietzsch, J. Henniger, S. Preusche, P. Mäding, J. Steinbach, *Appl. Radiat. Isot.* **2012**, 70, 602–608.
- [79] a) R. Přibil, *Analytical Applications of EDTA and Related Compounds*, Pergamon Press, Oxford, **1972**; b) G. Schwarzenbach, H. Flaschka, *Complexometric Titrations*, Methuen, London, **1969**.
- [80] a) Z. Otwinowski, W. Minor, HKL Denzo and Scalepack Program Package; Nonius BV: Delft, The Netherlands, **1997**; b) Z. Otwinowski, W. Minor, *Methods Enzymol.* **1997**, 276, 307–326.
- [81] A. Altomare, M. C. Burla, M. Camalli, G. Cascarano, C. Giacovazzo, A. Guagliardi, G. Polidori, *J. Appl. Crystallogr.* **1994**, 27, 435–435.
- [82] G. M. Sheldrick, SHELXL97, Program for Crystal Structure Refinement from Diffraction Data: University of Göttingen, Göttingen, **1997**.
- [83] G. M. Sheldrick, SHELXS97, Program for Crystal Structure Solution from Diffraction Data: University of Göttingen, Göttingen, **1997**.
- [84] P. Coppens, *Crystallographic Computing* (Eds.: F. R. Ahmed, S. R. Hall, C. P. Huber), Munksgaard, Copenhagen, **1970**, pp. 255–270.
- [85] A. L. Spek, PLATON, A Multipurpose Crystallographic Tool, Utrecht University, Utrecht, **2005**.
- [86] a) M. Kývala, I. Lukeš, International Conference Chemometrics 1995 (Pardubice, Czech Republic) July 3–7, **1995**, p. 63; b) M. Kývala, P. Lubal, I. Lukeš, IX. Solution Equilibria Analysis with the OPIUM Computer Program; Spanish-Italian and Mediterranean Congress on Thermodynamics of Metal Complexes (SIMEC 98) (Girona, Spain), June 2–5, **1998**. The full version of the OPIUM program is available (free of charge) on <http://www.natur.uni.cz/~kyvala/opium.html>.
- [87] *Scientist for Windows*, Version 2.01, Micromath Inc., Salt Lake City, **1995**.

Received: October 22, 2014

Published online on February 3, 2015